J Mater Sci (2013) 48:3027–3054
DOI 10.1007/s10853-013-7145-8

REVIEW

Electrospun fibers for tissue engineering, drug delivery, and wound dressing

Yi-Fan Goh · Imran Shakir · Rafaqat Hussain

Received: 28 August 2012 / Accepted: 7 January 2013 / Published online: 24 January 2013

Abstract Electrospinning, a technique well known for fabricating nanoscale fibers, has recently been studied extensively due to its various advantages such as high surface-to-volume ratio, tunable porosity, and ease of surface functionalization. The resulting fibers are extremely useful for applications in the fields of tissue engineering, drug delivery, and wound dressing. Since electrospun fiber mimic extracellular matrix of tissue in terms of scale and morphology, its potential to be used as scaffold is continuously explored by researchers, especially in the field of vascular, nerve, bone, and tendon/ligament tissue engineering. Besides morphology, physical, and chemical properties, electrospun scaffolds are often evaluated through various cell studies. Researchers have adopted approaches such as surface modification and drug loading to enhance the property and function of scaffold. This review gives an overview of some current aspects of various applications of electrospun fibers, particularly in biomedical fields, how researchers have enhanced electrospun fibers with different methods and attempted to overcome the inherent limitation of electrospinning by using novel techniques.

Y.-F. Goh
Department of Chemistry, Faculty of Science, Universiti Teknologi Malaysia, 81310 Skudai, Johor, Malaysia

I. Shakir
Department of Sustainable Energy, King Saud University, Riyadh, Saudi Arabia

R. Hussain (✉)
Ibnusina Institute for fundamental Sciences, Universiti Teknologi Malaysia, 81310 Skudai, Johor, Malaysia
e-mail: rafaqat@kimia.fs.utm.my

Introduction

Electrospinning, a process utilizing electrostatic forces to fabricate fibers, has been known since 1897 when the principle was first reported by Rayleigh [1], who first reported the electric charge of a liquid droplet required to eject the droplet to form smaller droplets. The first developmental milestone in electrospinning was achieved when Formhals patented the process in 1934 [2]. In 1966, a patent (Patent Number: 3280229) was granted to Simon [3] for producing patterned nonwoven fabrics using electrostatic force. Another milestone was the charged jet forming process discovered by Taylor in 1969 [4]. Numerous research groups have published work on electrospinning in the period 1970–1996, either exploring potential application or studying the electrospinning process itself [5–9]. The setup of electrospinning and the electrospinning process have recently been well discussed [10–13]. The three basic components of the electrospinning setup are high voltage DC power supply, syringe pump and grounded collector (Fig. 1). The syringe pump is used to force the solution or melt through a needle attached to the syringe with a controlled flow rate. When the high voltage is applied to the solution or melt, it induces a charge in the solution, resulting in a repulsive interaction between like charges in the solution, which increases with the electric field induced by high voltage. A Taylor [4] cone is formed when electrical forces in solution are balanced by surface tension. When the electrical forces become greater than the surface tension of the solution, a charged fiber jet is ejected from the Taylor cone and accelerates towards a grounded collector.

Apart from the geometry of the collector, there are many other controllable parameters which affect the formation of fibers during the electrospinning process. These can be categorized into three types:

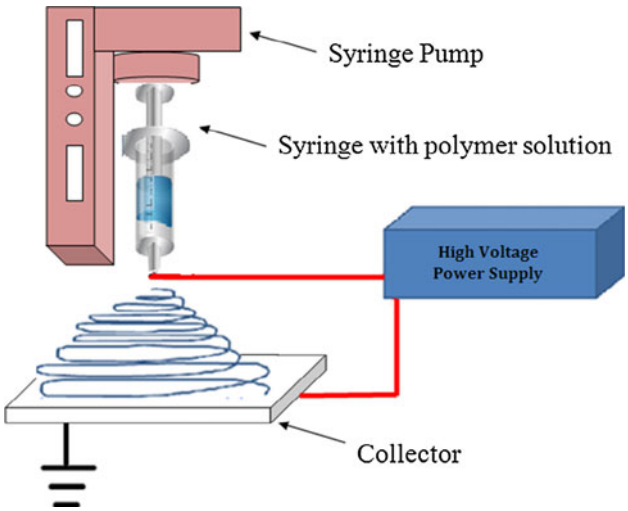

Fig. 1 Electrospinning setup

a) Solution parameters include conductivity, surface tension, and viscosity of the solution [14].
b) Process parameters include applied voltages [15], distance between tip to collector [16], flow rate [17], and electric field induced by the collector.
c) Ambient parameters such as temperature [18] and humidity [19] are often overlooked but are nevertheless important.

Electrospinning is the most reliable method known to produce continuous nanoscale fibers. Compared to other techniques such as phase separation [20] and self assembly [21], electrospinning has the advantages of producing continuous fibers, simplicity of process and most importantly, versatility in spinning a wide range of materials such as polymer, ceramic as well as composites into fibers ranging from nanometer to micrometer in size [22–26]. Nanofibers produced utilizing this technique possesses the characteristics of large surface-volume ratio, tunable porosity and ease of surface functionalization. These characteristics make nanofibers suitable for many applications, either in energy-related applications such as fuel cells [27], dye-sensitized solar cells [28], lithium-ion batteries [29], and supercapacitors [30] or biomedical applications such as affinity membranes [31], controlled drug release [32–34] tissue engineering [35–37], biosensors [38], and wound dressing [39].

Over the last decade, electrospinning of polymers has been under intensive investigation because of the versatility of electrospinning a wide range of natural and synthetic polymers. Commonly used natural polymers for electrospinning include collagen [40, 41], gelatin [42, 43], chitosan [44, 45], silk fibroin [40, 46], and chitin [47, 48], whereas synthetic polymers include polylactide [49, 50], polyglycolide [51, 52], and poly(ε-caprolactone) (PCL) [37, 42]. Electrospun copolymer fibers have also been explored because they enable the researchers to tailor the properties of the fibers by controlling the concentration of monomers. For instance, poly(methyl methacrylate) (PMMA), an engineering material with high mechanical strength has limited use because it decomposes at about 250–300 °C in air but by incorporating methacrylic acid in PMAA matrix, its degradation temperature has been increased by 80 °C [53].

Electrospinning has made possible the fabrication of ceramic fibers, these fibers are of high interest due to their high surface area to volume ratio, which offers potential application in many areas. A large number of research studies are focusing on making and improving ceramic nanofibers for various applications. The most recent examples include ZnO fibers targeted for gas sensors [54], dye-sensitized solar cells [55], hydrogen storage [56], photocatalysts [57]; CuO fibers aimed for dye sensitized solar cell [58], dye degradation [58], sensors [59]; TiO_2 fibers particularly dedicated to photocatalyst [60, 61]; SnO_2 fibers for use in toluene sensors [62], hydrogen sensors [63], and H_2S sensors [64]. Bioactive glass composed mainly of silicate, calcium oxide, and phosphorus oxide with various relative compositions is one type of ceramic that is well known for its biocompatibility, bioactivity, and osteoconductivity. However, it was not studied until 2006, when the first fabrication of bioactive glass nanofibers was reported [65]. Electrospinning of polymer–ceramic composites has long been the interest of many researchers because of its advantage over one-component matrix. By combining the two materials, the resultant electrospun composites gain the physical and chemical properties of the two materials, which often complement each other. For example, ceramics such as hydroxyapatite (HAp) has been incorporated into collagen to form composite nanofibers with the aim of improving mechanical strength while preserving the native nature of the collagen targeted for bone tissue engineering [66]. Bioactive glass has also been added to polymers such as PCL [67] and PLLA [68] to impart bioactivity to the synthetic polymer. Some other examples of polymer–ceramic composites nanofibers are chitosan/HAp [69], PLLA/HAp [70], PCL/HAp [71], and collagen/bioactive glass [72].

Only recent literature in electrospun nanofibers in the area of tissue engineering and wound dressing are discussed in detail here. Advances in vascular, nerve, bone, ligament, and tendon engineering are discussed in the section of tissue engineering. Recent approaches and focused aspect used in electrospinning community in recent years are explored, e.g., use of various types of surface modification of vessels in small diameter applications. Aspects such as fiber alignment, electrical stimulation, and growth factor incorporation are discussed in

nerve engineering. The feasibility of various combinations of polymer and ceramics composites system and their cellular response in bone and tendon/ligament engineering is extensively studied. Multifunctional fibers have been developed in wound dressing to achieve higher rate of healing. The current limitations of the electrospinning in tissue engineering and wound dressing are also identified and the most recent attempts to address these issues by using some novel techniques are described.

Biomedical application of electrospun nanofibers

Tissue engineering

The aim of tissue engineering is to restore or regenerate injured tissue by using various combinations of biomaterials, cells, and bioactive agents [73]. Isolated cells originating from a patient can be grown on a scaffold ex vivo followed by implantation at the injured site in the patient's body. Alternatively, scaffold can be directly delivered to the injured site of the patient to induce tissue formation in situ [74]. Apart from serving as a temporary and artificial extracellular matrix (ECM) for growing cells which degrade over time (Fig. 2b), scaffolds can be used as a reservoir to deliver bioactive agents to promote regeneration of the injured tissues [75]. Owing to the versatility of electrospinning such as spinning various materials and producing nanofibers with large-specific surface area that mimic natural ECM in terms of scale and structure, it has been used in the engineering of various tissues, for example, vasculature, nerve, bone, and tendon (Fig. 2a).

Vascular tissue engineering

Only clinically approved synthetic replacement materials for coronary artery in cardiovascular disease are expanded polytetrafluoroethylene (ePTFE) and Dacron®, which have been successfully used for large diameter vascular grafts. However, due to the thrombus formation, occlusion, and intimal hyperplasia, fabrication of small diameter (<6 mm) vascular graft remains a great challenge for researchers. This issue has become the main focus of interest for many recent research studies on electrospun vascular grafts [60, 76, 77]. Surface modification presents a potential approach to tackle this challenge. Researchers have enhanced endothelialization process by surface modification of electrospun nanofibers since endothelial cells (EC) exhibit antithrombotic properties [78]. EC capturing ligands have been used to achieve rapid endothelialization [79]. Use of a small-diameter nanofibrous vascular graft made of PCL [80] coated with an arginine-glycine-aspartic acid (RGD)-containing molecule named Nap-FFGRGD has been reported. This molecule of RGD and hydrophobic naphthalene groups can self assemble on the hydrophobic surface to form a RGD containing layer. PCL grafts and RGD–PCL grafts when implanted in rabbit carotid arteries for 2 and 4 weeks showed that the EC on the RGD–PCL were confluent and their alignment resembled the native vessel, whereas EC found on the PCL graft were randomly aligned. The endothelialization rates for RGD–PCL grafts (27.2 ± 11.5 and 51.1 ± 6.4 % at 2 and 4 weeks, respectively) were much faster than that of the PCL grafts (1.8 ± 1.1 and 11.5 ± 3.2 % at 2 and 4 weeks, respectively).

A polypeptide named hirudin has been conjugated to the surface of small diameter poly(*l*-lactic acid) (PLLA) by

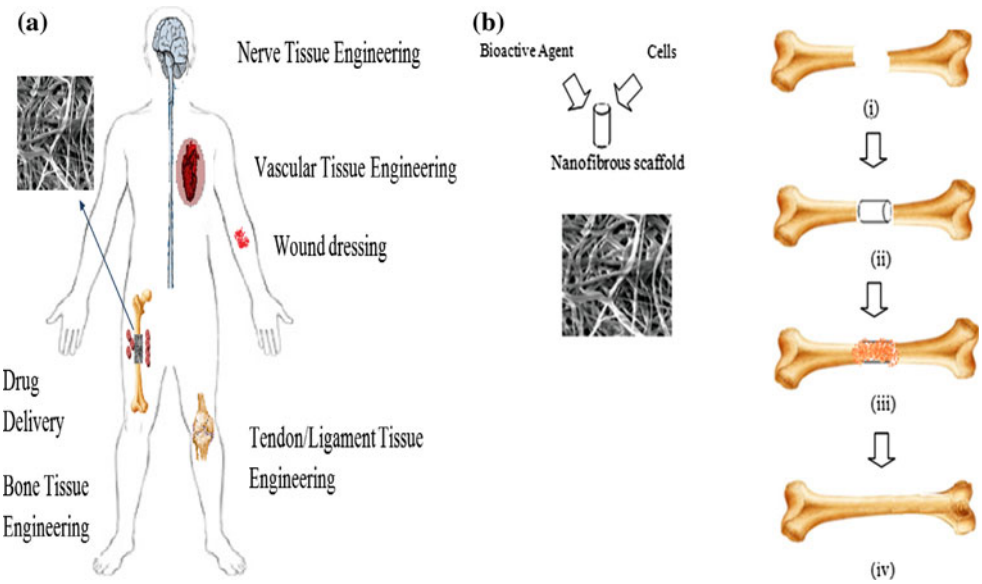

Fig. 2 **a** Biomedical application of electrospun fibers. **b** Concept of tissue engineering; (*i*) damaged bone, (*ii*) scaffold implanted into bone, (*iii*) new bone tissue formation on the scaffold, (*iv*) degradation of scaffold and complete regeneration of bone tissue

using an intermediate linker of poly(ethylene glycol) (PEG) [81]. Hirudin possesses blood anticoagulant properties whereas PEG helps to reduce platelet aggregation as well as immobilize hirudin. When untreated PLLA grafts, PEG-modified PLLA grafts and hirudin–PEG-modified PLLA grafts were implanted into the common carotid artery of rats for 1 month, the results showed that both PEG and hirudin improved the patency rate of the vascular graft. The hirudin–PEG-modified grafts were studied in vivo for another 5 months and as a direct result of this study six out of the seven grafts were later patented. All of the patented grafts exhibited complete endothelial coverage after 1 and 6 months of implantation. EC were aligned in the blood flow direction and morphologically resembled the endothelial cells in native arteries.

Apart from polypeptides [82, 83], proteins such as collagen [84, 85], fibronectin [86], gelatin [87], and hydrophobin [88] have also been used to modify graft surface to promote the growth of endothelial cells. Seeding of human coronary artery endothelial cells (HCAECs) onto the PLLA–PCL (70:30) nanofibrous tubular scaffold showed that the HCAECs were sub-confluent in just after 1 day and had spread well on the scaffold in 7 days, confirming that the collagen-coated PLLA–PCL scaffold promotes fast and stable in vitro endothelialization [84]. Figure 3 shows the macroscopic and microscopic nanofibrous structure of the tubular scaffold.

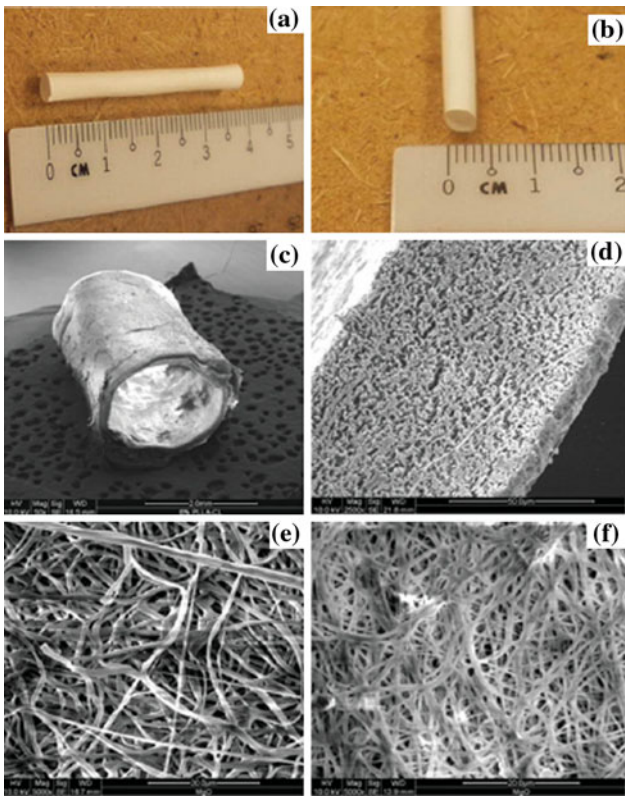

Fig. 3 **a**, **b** Macroscopic view of P(LLA–CL) tubular scaffold. **c** SEM images of 3D structure (×50). **d** Cross-section (×2,500). **e** Outer surface (×5,000). **f** Inner surface (×5,000) [84]

Anticoagulants may help to prevent thrombus formation caused by platelet deposition, thus allowing endothelial cells to grow fully on the lumenal surface of vascular graft. In this context use of sulfated silk fibroin scaffolds to improve the antithrombogenicity of the vascular grafts was reported [89]. Incorporation of sulfate and sulfonate groups into polymers can render them anticoagulant activity. EC and smooth muscle cells (SMC) cultured on the sulfated silk scaffold demonstrated good attachment and growth within 24 h. Result of gene and protein expression of markers showed better cellular function of EC and SMC on sulfated silk fibroin scaffold than the simple silk fibroin scaffold. Polysaccharide such as heparin [90–93] has also been used as anticoagulant and tool to immobilize growth factor [94] in vascular engineering. Various types of molecules used in surface modification of fibers are listed in Table 1.

Another approach to reduce thrombogenicity of a synthetic graft is by using a bioinspired phospholipid polymer, namely 2-methacryloyloxyethyl phosphorylcholine (MPC) or MPC-based copolymers. The use of 1.3-mm diameter conduit made from the fibrous blend of biodegradable poly(ester urethane)urea (PEUU) and poly(2-methacryloyloxyethyl phosphorylcholine-*co*-methacryloyloxyethyl butylurethane) (PMBU) in different weight fractions is known to exhibit better patency (67 %) than that of PEUU without PMBU (40 %), when planted in the rat abdominal aorta for 8 weeks [95]. Implantation of the immobilized phospholipid copolymer (70 mol % MPC and 30 mol % methylacrylic acid) on PEUU scaffold in rat abdominal resulted in larger patency (92 %) than for the nonimmobilized grafts (40 %). Reduced platelet deposition (tenfold) was observed for the surface-modified graft. Also the lumen of the surface-modified graft showed confluent and aligned EC suggesting that the scaffolds with MPC-based copolymers possess favorable anti thrombogenicity properties.

Above-mentioned studies provide insight into the in vivo performance of synthetic vascular graft over short span of time (8 weeks—6 months). To evaluate the performance of synthetic grafts over longer period of time the in vivo performance of PCL micro-, nanofibrous vascular scaffold in rat abdominal aorta replacement model for 1.5, 3, 6, 12, and 18 months was examined [96]. Although there was rapid and confluent endothelialization, intimal hyperplasia (growth of smooth muscle cells between endothelium and graft material) developed as early as 1.5 months after implantation and grew between 40 and 70 μm. The cell growth occurred significantly over the first 6 month and stabilized between 6 and 18 months. Calcification of

Table 1 Surface modification in vascular tissue engineering

Surface-modified/coated	Polymers	Remarks	References
Tripeptide	PCL	RGD layer promoted endothelialization; alignment of EC-resembled native vessels	[80]
Polypeptide	PLLA	The presence of hirudin, an anticoagulant improved patency rate; EC aligned in blood direction	[81]
Polypeptide	PU	Use of recombinant elastin-like polypeptide-4 (ELP4) mimicking native tropoelastin enhanced smooth muscle cell (SMC) adhesion and maintenance of cell numbers	[82]
Polypeptide	PCL	Recombinant human tropoelastin helped to reduce platelet attachment	[83]
Protein (collagen)	P(LLA-CL)	Fast and stable in vitro endothelialization	[84]
Protein (collagen)	P(LLA-CL)	Good spreading, viability and attachment of human coronary artery endothelial cells	[85]
Protein (fibronectin)	PLLC	Enhanced epithelium regeneration	[86]
Protein (gelatin)	PET	Improved spreading and proliferation of EC	[87]
Protein (hydrophobin)	PCL	Anti-CD31 antibody immobilized on the HFBI-coated PCL scaffolds promoted the attachment and retention of endothelial cells	[88]
Sulfonate group	Silk	Anticoagulant-improved antithrombogenicity; good attachment and growth within 24 h for EC and smooth muscle cells (SMC)	[89]
Polysaccharide	Silk	Heparin imparted antithrombogenicity while showed minimal inflammation in vivo	[90]
Polysaccharide	Chitosan/PCL	Heparin-promoted rapid induction of re-endotherlization	[91]
Polysaccharide	PLLA	Heparin was coated along with chitosan by electrostatic self-assembly techniques; better growth of endothelial vascular cells	[92]
Polysaccharide	PTFE	Heparin significantly reduced platelet adhesion and inhibited whole blood clotting kinetics	[93]
Polysaccharide	PCL/gelatin	Heparin-mediated delivery of platelet-derived growth factor-BB (PDGF-BB)	[94]
Phospholipid	PEUU/PMBU	Use of 2-methacryloyloxyethyl phosphorylcholine (MPC)-based polymers; larger patency and reduced platelet deposition observed	[95]

the graft, smooth muscle cells differentiated into chondrocytes at the interface between the graft and intimal hyperplasia. 54 ± 1 % of the graft length and 8.7 ± 5.5 % of the graft volume was also observed after 12 months. After 18 months, 86 ± 5 % of the graft length and 14.4 ± 1.9 % of the graft volume were calcified. Compact bone with viable osteocytes was also reported in some areas of the graft materials, moreover, although vascularization occurred rapidly upon implantation of the graft, progressive regression occurred over time (Fig. 4). Only a few capillaries remained in the graft wall after 18 months. This study demonstrated that the long-term in vivo behavior of the graft must be considered to determine the clinical suitability of the graft as some useful data and information could not be obtained through short-term implantation and in vitro test.

Nerve tissue engineering

Another interesting application of electrospun fibers is in the field of nerve tissue engineering. Owing to the ability of stem cells to differentiate into various specific cells, stem cells have been used in in vitro study of scaffold in nerve tissue engineering. Neuronal differentiation and neurite outgrowth and linkage to neighboring cells is observed when seeding and culturing the undifferentiated human embryonic stem cells on randomly distributed electrospun polyurethane nanofibrous scaffolds [97]. It is understood that highly aligned nanofibers are needed to prevent deviation of the axonal outgrowth on fibers from the natural axis of growth which may otherwise result in delaying axonal extension from one end to another in a scaffold [98]. The orientation of neurite grown in a PLLA scaffold was changed by crossing fiber (Fig. 5), thus suggesting that crossing fiber may have a detrimental effect on the directed axonal outgrowth [98]. Substrate topography is also known to affect the morphology of the stem cell, thus affecting its growth, survival, and differentiation of gene expression. Adult neural stem cells on aligned PCL fibers exhibited better neuronal differentiation compared to those on random fibers [99]. In another study the aligned poly(lactide-*co*-glycolide) (PLGA) fibers were able to guide the Schwann cells along their length and showed a better rate of cell proliferation than their randomly oriented counterparts. Besides this, the longitudinally oriented scaffold exhibit better deformability, slower degradation rate,

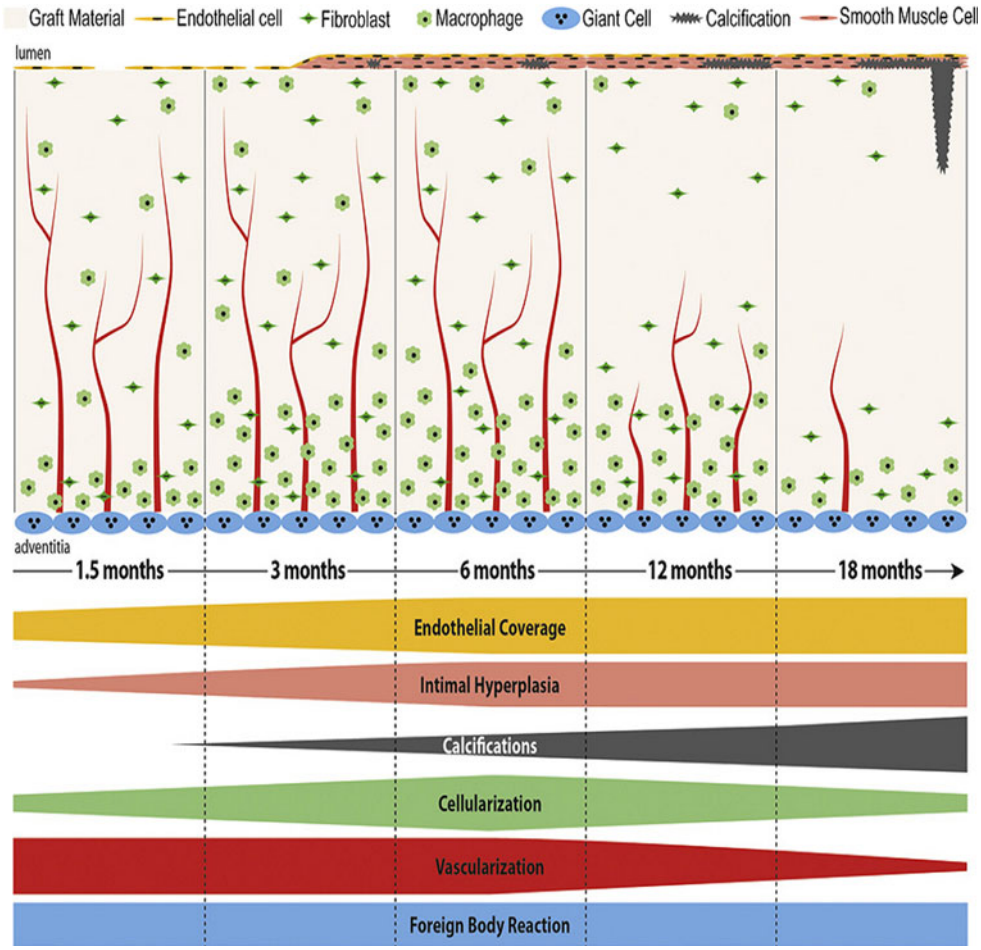

Fig. 4 Graphical representation of biological response of the vascular graft in vivo over time [96]

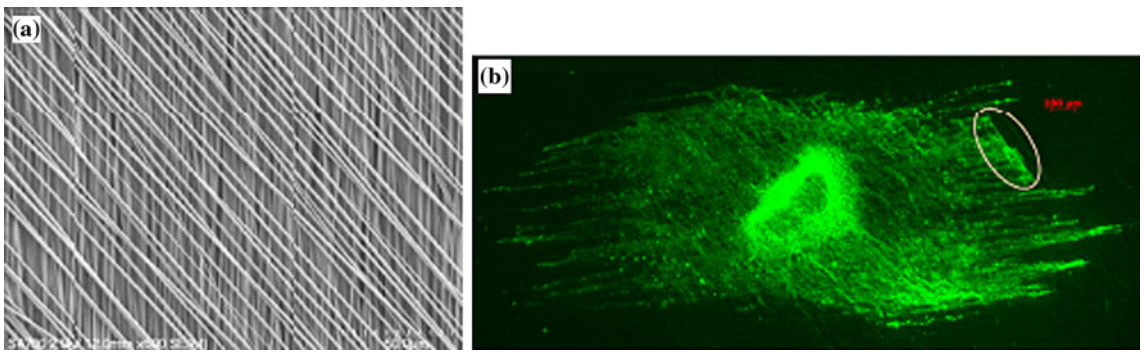

Fig. 5 **a** PLLA-aligned crossing fiber. **b** Immunostaining showing effect of crossing fiber on direction of neurite growth [98]

smaller pore size, and similar porosity to random fibers [39].

Scaffolds pre-seeded with cells play an important role in nerve tissue regeneration especially when defective gaps are longer than 30 mm. The cell sources can be olfactory ensheating cells, embryonic stem cells, Schwann cells, and mesenchymal stem cells (MSCs) [100]. MSCs have received special attention compared to other cell types because they are easily accessible. Researchers are still finding ways to enhance the neuronal differentiation of MSCs. They have found that the way of delivering induction factors and topographical cues of the matrix are essential in promoting the differentiation. MSCs seeded on the nerve growth factor (NGF) conjugated on the surface of the PCL nanofibrous mesh through the use of amine-terminated poly(ethylene glycol) exhibited higher expression levels of neuronal differentiation markers such as nestin, tubulin βIII, and map2 than the NGF-absorbed

mesh. Greater elongation of stem cells for aligned nanofibers than the random nanofibers with NGF is also known [101]. Sustained drug delivery of retinoic acid from the 3D-aligned PCL nanofibers is recognized to promote better neural marker expression when compared with tissue culture polystyrene [102].

The type of incorporated drugs for nerve regeneration depends on the strategy used and the local environment of the site of injury. The formation of glial scars after spinal cord injuries always inhibited the regeneration of neurons. Since chondroitin sulfate proteoglycans (CSPGs) is a major component of glial scars, chondroitinase ABC (ChABC) which can digest CSPGs is often selected to treat spinal cord injuries. Electrospun collagen fibers have been used to deliver ChABC locally in a sustained manner for up to 32 days [103]. This period matches well with the in vivo CSPGs expression kinetics, which peaks at 2–4 weeks after spinal cord injury. Besides CSPGs, astrocytes in the glial scar after nerve trauma are reported to be detrimental to the regeneration of nerve [104]. Highly aligned electrospun fibers with different amounts (10, 20 w/w%) of an anti-metabolite 6-aminonicotinamide (6AN) have been shown to reduce the metabolic activity of astrocytes. Culturing of dorsal root ganglia (DRG) on the scaffolds showed no significant difference in neurite extension for control and 10 % 6AN fibers, however, the metabolic activity of astrocyte in 6AN fibers was significantly reduced [105]. In a different study, electrospun silk fibers were used for optic nerve regeneration, where functionalized aligned nanofibers with brain-derived neurotrophic factor (BDNF) and ciliary neutrophic factor (CNTF) were used [106]. Both factors are often secreted from the glial cells which are activated after optic nerve trauma. The results showed that silk/BDNF/CNTF>silk/CNTF>silk/BDNF>silk were better in terms of the ability to improve the rate of neurite extension.

One emerging area in neural tissue engineering is the use of electrical stimulation to promote neurite growth. In vitro electrical stimulation of the nerve stem cells seeded on PLLA/polyaniline (PANI) nanofibrous scaffolds with an electric field of 100 mV/mm for 60 min resulted in the increase in length of neurite outgrowth by 60 % compared to the one without electrical stimulation (24 ± 4 vs 15 ± 3 μm) [107]. Study of synergistic effect of electrical stimulation and topographical cues on the neurite growth of DRG on PCL-pyrrole core-sheath nanofibers [108] showed that the aligned nanofibers after electrical stimulation exhibited greater maximum neurite length (2542 ± 171 vs 1723 ± 339 μm) compared to their counterparts without electrical stimulation. Similarly, random nanofibers also exhibited greater maximum neurite length (1733 ± 141 vs 946 ± 146 μm). It was therefore, concluded that the electrical stimulation has a better effect on random nanofibers than the aligned one (83 vs 47 % increase). This was attributed to the growth limitation of neurites over a fixed period of time and a lower basis in the random fibers without stimulation [108]. In another study a conductive PLGA nanofibers coated with polypyrrole were prepared and cultured with rat pheochromocytoma 12 (PC12) cells on the fibers. The results showed an increase in neurites length from 12.7 to 18.9 μm for aligned fibers and 14.9 to 21.1 μm for random fibers after electrical stimulation. It was also suggested that a lower electrical field may be more favorable for neurites growth [109]. Both studies demonstrated that synergistic effect of electrical stimulation and topographical cues have impact on the neurites growth on nanofibers.

Conductive nature of a polymeric scaffold is a pre-requisite for electrical stimulation, therefore, conductive polymers such as polypyrrole (PPy), PANI, poly(3,4-ethylenedioxythiophene) (PEDOT) or even carbon nanotubes (CNT) are often used. PPy and PANI are the most extensively studied conductive polymers [35], however, they are not conductive in their base form so they must be doped with acids such as camphor sulphonic acid (CSA) or hydrochloric acid (HCl) to be conductive. Due to the poor mechanical properties and low electrospinnability (low solution viscosity), PANI has been mixed with gelatin [110], poly(l-lactide-*co*-ε-caprolactone) [111], and PMMA [112] to achieve desired properties. Similar to PANI, PPy has poor solubility in common solvents, making it difficult to be processed. Electrospinning of PPy can be achieved by using poly(ethylene oxide) (PEO) as carrier, PEO can be removed through ethanol extraction after the electrospinning but this can adversely affect the morphology of the fibers [113]. Instead of simple blending, in situ polymerization of pyrrole on the surface of electrospun PLLA fiber has been performed [114]. Conductivity and porosity of the PLLA/PPy fiber can be optimized through the manipulation of polymerization time, temperature, and dispersion method. Vapor phase polymerization method can be used to deposit PPy on poly(styrene-β-isobutylene-β-styrene) fibers, which supports attachment and growth of P12 cells [115]. Besides conductive polymers, piezoelectric polymer such as polyvinylidene fluoride–trifluoroethylene (PVDF–TrFE) [116, 117] has been explored in the field of nerve regeneration due to its electrical properties. A piezoelectric material is characterized by the generation of electricity in response to a mechanical stress. The presence of TrFE in the copolymer is important as steric hindrance forces PVDF in all-*trans* configuration, imparting its piezoelectric properties. Series of random and aligned PVDF–TrFE micro and nano-sized nanofibers, PVDF nanofibers, and PVDF-TrFE powders were prepared to study their piezoelectric properties. Piezoelectric crystal phase (β phase) was studied by using thermally stimulated depolarization

current (TSDC), XRD, and FTIR. The results showed that PVDF nanofibers exhibited no presence of piezoelectric β phase crystals whereas all PVDF–TrFE were found to have the β phase crystals and supported the attachment and growth of dorsal root ganglion (DRG) neurons [116]. Annealing nanofibers at 135 °C for 96 h further enhanced their piezoelectric properties. List of polymers and their use in nerve tissue engineering are summarized in Table 2.

Bone tissue engineering

Since ECM of bone is mainly made of collagen (organic component) and HAp (inorganic component), composite scaffolds for bone tissue engineering are subject of countless investigations. The most recent examples include HAp/PLLA [70], beta-tricalcium phosphate (β-TCP)/poly(ε-caprolactone) (PCL) [118], HAp/PLLA/collagen [119], HAp/PLLA/poly-benzyl-L-glutamate (PLBG)/collagen [120], and β-TCP/PCL/collagen [121]. Micro-sized HAp particles perform better than nano-sized HAp particles in terms of cell proliferation and differentiation of rat osteosarcoma cells on the composite scaffold [70]. Whereas the mechanical strength of β-TCP/PCL composite fibers is affected by the relative amount of β-TCP [118]. Incorporation of poly-benzyl-L-glutamate (PLBG), a polypeptide into the composite fibers is known to improve cell adhesion and differentiation, this increase is attributed to the osteoconductive properties of HAp and calcium-binding ability of PLBG. The addition of collagen can improve the water uptake of the composite fibers, which may help to prevent the loss of body fluid and nutrients in vivo [121]. Synergistic effects of collagen (providing extra cell recognition site) and HAp (chelating agent for mineralization) can stimulate better growth of human fetal osteoblasts and 57 % higher mineral deposition on PLLA/collagen/HAp nanofibers than the PLLA/HAp nanofibers [119]. The pore size of the PLLA/collagen/HAp fibrous scaffold was not reported but it is expected that the excessively small pore size within the polymer matrix will prevent efficient cellular infiltration. Phipps and co-workers [122] constructed PCL/collagen/HAp nanofibrous scaffolds by using three methods: limited protease digestion, reduction of fiber packing density and inclusion of sacrificial fiber of PEO to increase the pore size of the scaffolds. They reported that the PEO sacrificial fibers were the most effective among the three methods to increase the pore size. Enhanced infiltration of MSCs into the scaffolds was observed with this method. It is clear that by modifying the sample preparation method with electrospinning, the properties of the scaffolds can be fine-tuned. This point was further strengthened when sol–gel processing method combined with electrospinning was used to produce gelatin–siloxane fibrous mats for potential use as scaffold in bone tissue engineering [123]. Moreover, self-assembling peptides coupled with RGD and mixed with PEO followed by electrospinning can provide biochemical adhesion

Table 2 Electrospun polymer and some aspects in nerve tissue engineering

Issues	Polymers	Remarks	References
Alignment fiber architecture	PLLA	Crossing fiber inhibited axonal outgrowth of neurite	[98]
	PCL	Adult neural stem cells on aligned fiber showed better neuronal differentiation	[99]
	PLGA	Better growth rate of Schwann cells on aligned fiber.	[39]
Stem cell based regeneration	Polyurethane	Human embryonic stem cells	[97]
Differentiation of Mesenchymal stem cells	PCL	Fiber surface conjugated with nerve growth factor (NGF)	[101]
	PCL	Sustained release of retinoic acid	[102]
Glial scars	Collagen	Sustained release of chondroitinase ABC (ChABC)	[103]
Glial scars	PLLA	Anti-metabolic 6-aminonicotnamide (6AN) reduced the metabolic activity of astrocytes	[105]
Glial scars	Silk	Functionalized fiber with brain-derived neutrophic factor (BDNF) and ciliary neutrophic factor (CNTF)	[106]
Electrical stimulation	PLLA/PANI	Nerve stem cells	[107]
	PCL/pyyrole	Core-sheath nanofibers, dorsal root ganglia (DRG)	[108]
	PLGA/ pyyrole	Rat pheochromocytoma 12 (PC12) cells	[109]
Conductive polymer	Polypyrrole/ PEO	PEO-facilitated electrospinning	[113]
	PLLA/ polypyrrole	In situ polymerization of polypyrrole	[114]
Piezoelectric polymer	PVDF-TrFE	Dorsal root ganglion (DRG)	[116]

signals which can interact with cell receptors and support better growth and differentiation of human osteoblast cells [36]. The above examples have shown that the functionality of a composite scaffold for bone tissue engineering can be affected by the size of particles incorporated, relative amount, porosity, processing method as well as the use of additional polymer.

Stem cell-based regeneration of defected bone tissue has aroused interest of many scientists due to its self-renewing ability to differentiate into a wide range of specialized cell lineages, including osteoblasts and chondrocytes, adipocytes, endothelial cells, fibroblasts, myocytes, and tenocytes [124]. Adult stem cells such as human mesenchymal stem cells (hMSCs) [125], adipose-derived stem cells [120], and umbilical cord stem cells [126] have been targeted for use in bone tissue engineering. Among them, hMSCs are the most used source in bone tissue engineering as they can be readily derived from human bone marrow. Surface coating of bioactive molecules can provide biochemical cues to MSCs to grow on a polymer fibrous scaffold [127, 128]. Electrospinning of poly(L-lactide) fibers followed by immersion in an aqueous solution of 3,4-dihydroxyphenethylamine (dopamine) to furnish polydopamine-coated PLLA (PD-PLLA) fibers can result in an increase in alkaline phosphatase (ALP) activity after 7 days of culturing of hMSCs when compared with pure PLLA fibers (1.74 ± 0.14 vs 0.97 ± 0.07 nmol/DNA/30 min). Besides this, the expression levels of runt-related transcription factor 2 (RUNX2), ALP, bone sialoprotein (BSP) gene, and angiogenic marker interleukin 8 (IL-8) can also be significantly enhanced by using PD-PLLA fibers [127]. All this data shows that the polydopamine can stimulate the initial osteogenic differentiation of hMSCs. The incorporation of drugs which can induce and support osteogenic differentiation of hMSCs into fibrous bone graft is an attractive approach [129, 130], and it is even more promising when fibers electrospun by coaxial electrospinning exhibit controlled release of drugs, thus achieving optimal dosages over a desired period. Loading of poly(L-lactide-*co*-caprolactone) (PLLACL) and PLLACL/collagen nanofibers with bone morphogenetic protein 2 (BMP2) and dexamethasone (DEX) by blending and coaxial electrospinning was used to study the osteogenic differentiation of hMSCs (ALP activity) and immunocytochemical staining for osteocalcin [131]. The researchers involved in the study reported that the osteogenic differentiation is affected by duration of exposure to BMP2 and DEX and their release profile, which in turn is related to the techniques applied for the fabrication of the scaffolds, i.e., blending or co-electrospinning and the distribution of drugs in fibers. Co-electrospun fibers were found to possess better controlled release profile for the two drugs than the blended fibers, hence more favorable for osteogenic differentiation. This was evident by the weaker osteocalcin expression shown by the blended fibers. Fiber alignment alone does not have a significant impact on the osteogenic differentiation of MSCs. The induction effects of fiber alignment in the presence of inductive adepogenic or osteogenic chemical factors are negligible, indicating that such effects can be ignored, especially inside the body, where the environment is changing dynamically due to the producing cells and deposited ECM [132]. However, a recent study reported that fiber alignment as well as diameter strongly influence the morphology of MSCs [133]. Indeed, differentiation of MSCs cells can be directed by physical factors such as patterned microstructure [134, 135], mechanical stimulation [136] or surface roughness [137], even without the use of any biological and chemical factors.

Incorporation of nano-sized HAp (nHAp) into polymeric fibers has been shown to enhance osteogenic differentiation and promote adhesion and proliferation of MSCs [138, 139]. ALP activity, expression of genes associated with osteogenic differentiation such as ALP, bone sialoprotein, and osteocalcin on the PLGA/nHAp fibers were enhanced by the presence of nHAp [140]. The ALP activity of cells on PCL fibers with different amount of nHAp (0–50 wt%) exhibited order of: PCL/50 % nHAp>PCL/25 % nHAp>PCL [141]. Elemental composition analyses (EDX) of calcium and phosphorus contents also showed the same pattern of order which led to the conclusion that higher concentration of nHAp resulted in enhanced MSCs differentiation into osteoblasts. nHAp also promoted mineralization of hMSCs, this was in agreement with the work of Lee and co-workers [140]. Both of the above examples involved blending nHAp directly with polymer prior to electrospinning which resulted in poor nHAp dispersion in polymer matrix, i.e., agglomeration of nHAp particles occurred on the fiber surface. γ-Glycioxypropyltrimethoxysilane (A-187), a coupling agent was used to pre-surface treat hydroxyapatite particle to enhance their dispersion in fibers [132]. TEM images (Fig. 6a) showed the agglomeration of HAp needle-like particles in nontreated HAp/PCL fiber, whereas HAp treated with A-187 was well dispersed on the PCL fiber. Mechanical properties such as tensile strength and Young's modulus of the fibers were improved from 1.19 to 4.86 and 1.19 to 7.77 MPA, respectively; indicating that the dispersion of HAp affects mechanical performance of a composite fiber. In vitro activity of the fibers was assessed in 1.5 simulated body fluid (1.5SBF), where no apatite formation was observed for PCL fibers after 7 days. However, PCL fibers containing A187-treated HAp and nontreated HAp showed deposition of apatite along the fiber axes as early as after 3 days of immersion (Fig. 6b) thus confirming that

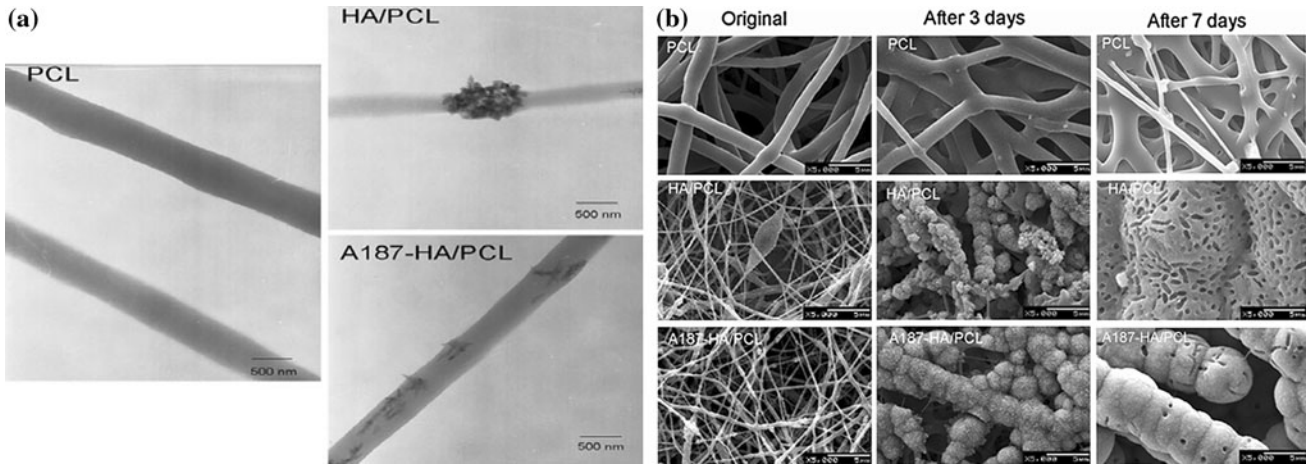

Fig. 6 **a** TEM images of PCL, HAp/PCL, and A187-HAp/PCL. **b** SEM images of fiber before and after immersion in 1.5SBF [132]

polymeric fibers-containing HAp are promising candidate for guided bone regeneration.

Other than a method to investigate in vitro bioactivity, SBF serves as an excellent alternative to perform biomimetic mineralization of fibrous structures. However, SBF is sometimes considered to be too time-consuming as it can take up to several weeks to give reliable results during which polymeric structure may start to degrade. Therefore, a new rapid method was developed in which calcium phosphate is electrodeposited onto the polymeric fibers. Deposition of PLLA nanofibers on the surface of metallic templates before electrodeposition is performed to obtain a calcium phosphate coating within 1 h [142]. The authors studied the effect of parameters such as fiber diameter, solution temperature, deposition voltage and time on the chemical composition, topography, and deposition rate of the calcium phosphates. For instance, as shown in Fig. 7, at 3 V and 60 °C, sparse flower-like structures (b) having diameter of about 4 μm appeared on the fiber surface after 15 min. It grew to about 8 μm in diameter (c) after 30 min and a dense flake-like network was formed after 1 h (d). The ALP activity of pre-osteoblast MC3T3-E1 cells on PLLA fibers treated with electrodeposition was greater than that of the nontreated fibers, showing that calcium phosphate coating on the fibers promote osteoblastic differentiation of the cells. Since surface topography and roughness of calcium phosphates have an impact on proliferation and differentiation of human bone cells, this technique is considered promising and worthwhile to use.

Bioactive glass is another popular ceramic material used in bone-related biomedical applications. One added advantage of silica-based bioactive glass over HAp is its higher bone-bonding ability [143] and silicon, which has been proven to be integral for in vivo bone formation [144–146]. The first kind of bioactive glass, called Bioglass® 45S5 was synthesized by Hench et al. [147] roughly 40 years ago. The Bioglass® consisted of 4 components—45 % SiO_2, 24.5 % CaO, 6 % P_2O_5, and 24.5 % Na_2O [148]. Bioactive glass with other composition such as binary system—SiO_2, CaO [149–151] and ternary system—SiO_2, CaO, P_2O_5 [152] are also widely studied due to their good bioactivity, osteoconductivity, and osteostimulative properties [153]. They have been used or have found potential application in bone-related biomedical application such as bone graft or filler [154, 155], dental [156], craniomaxillofacial applications [157, 158], and implant coatings [159, 160]. However, its fibrous form was not studied until 2006, when Kim et al. [65] first reported the fabrication of bioactive glass nanofibers, followed by other researchers [161–165].

Sol concentration is a dominant factor in controlling the diameter of the bioactive glass nanofibers, in general higher sol concentrations result in the formation of fibers with larger diameter [65]. Although, the diameter decreases with reducing concentration but extensive beads formation often results at low sol concentrations. Fibers cannot be produced without polymer addition due to the lack of sufficient chain entanglement which is not possible by the Si–O network of bioactive glass sol. Addition of a pluronic surfactant, P123, can help to balance the electrostatic force and surface tension of solution and possibly reduce the diameter of the fibers [161]. Mesoporosity in bioactive glass can enhance the formation of carbonated hydroxyapatite (cHAp) compared to the conventional bioactive glass [166]. Lu et al. [162] reported the formation of mesoporous microfibers but the pore size was uncontrollable. Therefore, efforts were made to synthesize controllable nanoporous, bioactive glass nanofibers by using a nonionic triblock copolymer–homopolymer, i.e., pluronic P123-polyethylene oxide (P123-PEO), as a co-template [164]. It was observed that the larger pore size resulted in smaller specific area and pore volume. Thermogravimetric (TGA) analysis revealed

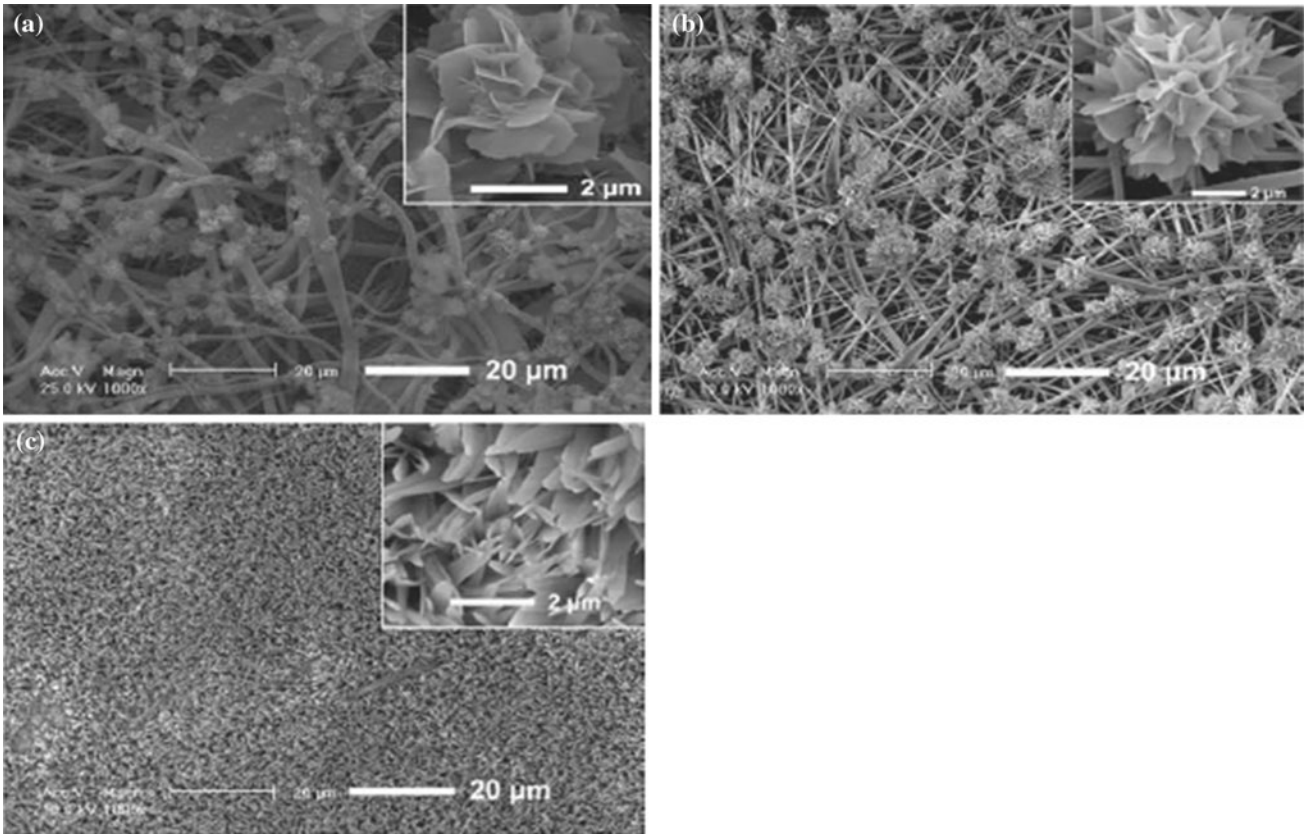

Fig. 7 SEM micrographs of PLLA scaffolds; deposition voltage: 3 V, temperature: 60 °C, deposition time: **a**15, **b** 30, and **c** 60 min [142]

that the homogeneity of bioactive compositions in the fiber matrixes became better with decrease in the diameter of the pores. Bioactivity of the nanofibrous bioactive glass can be enhanced by fabricating bioactive glass nanotubes by using a coaxial electrospinning technique. The rate of biomineralization process in the nanotubes is greater than that of nanofiber because an apatite layer is formed on both outer and inner surfaces of the nanotubes while it can only occur on the surface of the nanofibers [165].

Adding nanofibrous bioactive glass of composition $70SiO_2{\cdot}25CaO{\cdot}5P_2O_5$ into PCL membrane, the bioactivity of the fibers was enhanced as the apatite layer was rapidly formed on the surface when immersed in an SBF solution. Furthermore, osteoblastic cells attachment (MC3T3-E1) was higher on the nanocomposite membrane than the pure PCL membrane [67]. These results confirmed that the bioactive glass fibers are osteogenic stimulant with potential use in bone regeneration field. Excellent biocompatibility of the nanofibrous bioactive glass was further confirmed when implantation of PCL, matrix incorporated nanofibrous bioactive glass scaffolds in Sprague–Dawley albino rats-exhibited good biocompatibility and bone-forming ability [167]. In contrast to the above methods, [67, 167] where nanofibrous bioactive glass was mixed with PCL to form a film, a nanofibrous composite scaffold was prepared by first crushing the nanofibrous bioactive glass to form nanoparticulate matter, then mixed with polylactic acid followed by electrospinning [68]. Formation of an apatite layer was reported after 3 days of immersion in SBF. Pre-osteoblastic cell culture also showed good cellular adhesion and proliferation on the bioglass fibrous scaffold. Tables 3 and 4 summarize how researchers have adopted different approaches to enhance MSCs differentiation and the combination of different polymers with bioceramics for use in bone tissue engineering.

Tendon/ligament tissue engineering

Electrospinning has also found application in tendon/ligament tissue engineering. Tendons are fibrous connective tissues that connect muscles to bones whereas ligament connects bone to bone. Their ECMs primarily consist of collagen type I, but other materials have also shown potential for use in scaffolds. Use of *Antheraea pernyi* silk fibroin as a raw material to electrospin a tendon scaffold was reported. The scaffold was evaluated in vitro and in vivo by studying the growth of tenocytes on scaffolds and the recovery of tendon tissue in New Zealand white rabbits with a gap defect in their Achilles tendon. In vitro

Table 3 Some approaches to enhance MSCs differentiation and bioactive materials used in bone tissue engineering

Approaches to enhance differentiation of MSCs	Polymers	Findings	References
Surface coating	PLLA	PLLA coated with polydopamine showed higher ALP activity and expression level of bone-related gene	[127]
Surface coating	PCL	Significantly greater attachment and spreading of hMSCs were observed on nanofibers coated with peptide amphiphile containing cell adhesive ligand (RGDS)	[128]
Drug loading	PCL	Release of DEX induced an increased concentration of alkaline phosphatase and deposition of a mineralized matrix	[129]
Drug loading	PCL/gelatin	Stromal cell-derived factor-1α (SDF-1α) significantly induced stimulated chemotactic migration of BMSCs in vitro and sixfold increase in the amount of bone formation compared to control	[130]
Drug loading	PLLACL	Co-electrospun fibers loaded with BMP2 and DEX showed higher osteoclacin expression than blended fibers	[131]
Fiber alignment	PHBHHx	Fiber alignment alone had no significant effect on osteogenic potential of MSCs	[132]
Fiber alignment	Silk Fibroin	Fiber alignment exhibited a strong influence on the morphology of MSCs; smaller diameter scaffolds are more favorable for the growth of MSCs	[133]
Patterned microstructure	PLLA-PCL	Significant up-regulation of several myogenic markers associated with for hMSCs cultured on the scaffold with narrow microchannels	[134]
Patterned microstructure	PCL	ALP concentration values increased progressively with time in the culture of BMSCs and progressive expression of specific osteoblastic glycoproteins; microtopography controlled the deposition of mineralized extracellular matrix along the pre-defined fiber direction	[135]
Fiber alignment/Mechanical stimulation	PLGA	Scaffold alignment and optimized mechanical stimulation, are sufficient to drive MSC differentiation, without the need for additional chemical stimuli	[136]
Surface modification	PEOT/PBT	Significant upregulation of bone sialoprotein and osteonectin expression on oxygen plasma treated fibres compared to untreated fibres	[137]
Addition of HAp	PCL	Higher content of HAp resulted in higher ALP activity	[126]
Addition of HAp	Peptide amphiphile	Enhanced osteogenic differentiation of hMSCs by HAp nanoparticles-reinforced peptide amphiphile nanocomposite matrix	[138]
Addition of HAp	PLLA	Biphasic scaffold coated with HAp/PLLA exhibited significantly increased proliferation of MSCs	[139]
Addition of HAp	PLGA	Higher content of HAp resulted in greater differentiation of hMSCs	[140]

Table 4 Combination of different polymers with bioceramics

Bioceramics particles/ polymer	Bioceramics nanofiber		
HAp/PCL	–	HAp-dispersed homogenously within fiber, fiber-induced apatite formation in SBF	[132]
PLLA	–	Electrodeposition of apatite layer on fiber promoted osteoblastic differentiation	[142]
–	Bioactive glass	First reported the fabrication of bioactive glass in fiber form	[72]
–	Bioactive glass	Studied effects of electrospinning parameters on fiber	[161]
–	Bioactive glass	Mesopores in fibers enhanced bioactivity	[166]
–	Bioactive glass	Nanoporous fibers with controllable porosity size were made	[65]
–	Bioactive glass	Bioactive glass nanotube was made by coaxial electrospinning	[165]
PCL (film)	Bioactive glass	Higher cell adhesion on PCL membrane blended with nanofibrous bioactive glass	[67]
PCL (film)	Bioactive glass	Good bone-forming ability in vivo in Sprague–Dawley albino rat	[167]
PLLA (fiber)	Bioactive glass	Apatite formation after 3 days of SBF, good pre-osteoblastic cell adhesion and growth	[68]

results showed that tenocytes grew and proliferated on the scaffold whereas after 16 weeks of in vivo implantation, uniform, and well-oriented bundles of collagen fibers in the neo-tendon tissue were formed [168]. Apart from tendon cells such as tenocytes, MSCs have also been extensively used to evaluate the biocompatibility of a scaffold used in

tendon/ligament tissue engineering. These cells have the ability to differentiate into tendon/ligament fibroblasts [169–172]. The incorporation of basic fibroblast growth factors have been incorporated and randomly distributed within PLGA nanofibers [173]. The alignment of fibers should also be considered when designing a tendon scaffold as the expression of tendon-specific genes were far higher in human tendon stem/progenitor cells growing on aligned nanofibers than in those on randomly oriented nanofibers in both normal and osteogenic media. Moreover, the aligned and randomly oriented nanofibers have different properties in terms of osteogenesis-inducing ability and the morphology of the resulting cells [174]. The alignment of electrospun fibers has also been known to affect ECM production ability of human ligament fibroblast [175]. Some studies suggest that crimp-like microstructure within electrospun scaffolds provide a better geometric microenvironment for ECM production by fibroblasts [176, 177]. Homogenous scaffolds may be good enough for tendon or ligament tissue regeneration, but not for interfaces such as tendon–muscle [178] or ligament–bone [179] because the two tissues have different requirements in terms of porosity, compliance, and mechanical properties. Therefore, co-electrospinning is used to fabricate scaffolds that serve the functions of two tissues or mimic the properties of the interface. Co-electrospinning of PCL/collagen and PLLA/collagen fibers onto opposite sides of a mandrel to produce a dual scaffold is known. Regional variations in mechanical properties were observed in the scaffold and the strain profiles had similar trends to those of the native muscle–tendon junction [178]. Graded scaffolds with different tensile moduli [179] or mineral contents [180] along the length of the mesh can be fabricated by co-electrospinning for use in ligament–bone interface.

Recent development in tendon/ligament tissue engineering saw the use of hybrid scaffolds in which electrospun fibers are combined with knitted structure to create a scaffold [181, 182]. Such scaffolds explored the mechanical properties of knitted structures and the topographical cues of electrospun fibers which fulfill the mechanical requirement for tendon/ligament graft as well as support cell adhesion, proliferation, and differentiation. The composite scaffold made from silk-knitted structure coated with poly(L-lactic-*co*-ε-caprolactone) (PLCL) microfibers had an elastic modulus of 150 MPa which is close to native tendon and ligament modulus of 50–100 MPa. Seeding efficacy of rat MSCs on the hybrid scaffold was also improved compared to that of the knitted structure not coated with microfiber. Immunostaining showed that collagen types I and III were present in tendon/ligament tissue after 1 week of cell culturing [181]. In another study, degummed knitted silk microfibrous scaffold coated with PLGA nanofibers was loaded with fibroblast growth factor (bFGF) (Fig. 8a, b). This growth factor promoted tenogenic differentiation of stem cells into tendon/ligament fibroblasts [182]. bFGF can be incorporated into fibers by coaxial electrospinning and blending, both showing sustained release from fiber, but increased collagen production and better fibroblast differentiation [183], activation of tyrosine phosphorylation signaling within seeded BMSCs [173] were shown in blended PLGA fibers. Rabbit BMSCs proliferated well on PLGA nanofiber as well as on the knitted silk microfibers. Cell viability was higher in bFGF-loaded PLGA/silk than PLGA/silk scaffold throughout cell culturing period of 21 days. Expression levels of type I and III collagens were also higher for bFGF-loaded PLGA/silk scaffold in day 14. The failure load of the BMSC-seeded scaffold after 3 weeks possessed failure load of 83 ± 3.5 N which is close to that of native rabbit ligaments (88–132 N). The nanofibers/knitted microfibrous scaffold preserved the mechanical properties and at the same time promoted stem cells adhesion, proliferation, and tenogenic differentiation, suggesting great potential use in regeneration of tendon/ligament tissue. List of different polymers used in tendon/ligament tissue engineering is presented in Table 5.

One of the major limitations of electrospun fibers is the small pore size which limits cellular infiltration, inhibit exchange of nutrient and waste with surrounding environment as well as prevent vascularization [184, 185]. This inherent characteristics greatly limits the potential use of electrospun fibers in tissue engineering as the growing cells should infiltrate into the fibrous structure and produce ECM to take over the structural role of fibers which will degrade over time. Conventional electrospun fibers have pore size of only a few or even <1 μm in diameter, but pore sizes of >300 μm has been recommended to facilitate cell growth and vascularization in bone [186] while human dermal fibroblast was reported to prefer pore size of 6–20 μm [185]. In most cases, cells are reported to adhere and grow well only on the 2D surface. There have been many efforts to increase the pore size of electrospun fibers; this includes addition of salt [187], cryogenic electrospinning [188], reducing fiber packing/density [189], inclusion of sacrificial fibers [190], photopatterning [191], or ultraviolet radiation treatment [192]. The inclusion of sacrificial fibers is found to be the best method to enhance cellular infiltration among limited protease digestion and reduction of fiber packing [122]. Besides this, pore size and porosity can be changed by manipulation with the flow rate during electrospinning process [193] or using various patterned collector [194]. Recently, femto second laser ablation was used to tackle this problem [195]. Various combinations of structured holes with diameters 50, 100, and 200 μm at the spacing of 50 and 200 μm between adjacent holes was successfully fabricated by manipulating laser energy and

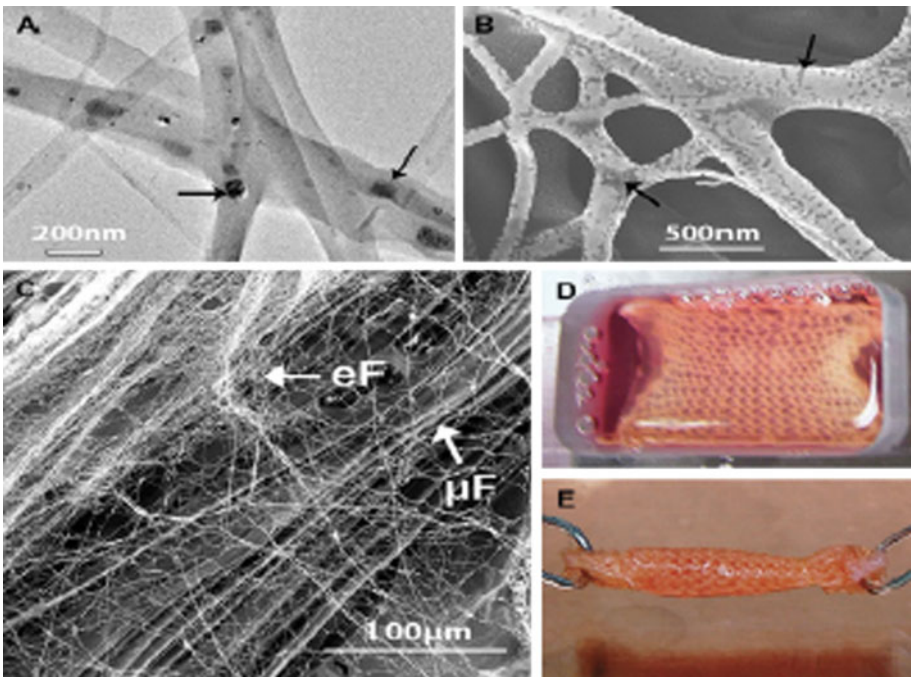

Fig. 8 **a** TEM image. **b** SEM image, *black arrow* indicates the presence of protein. **c** SEM image of (eF) PLGA nanofibers and (μF) microfibrous-knitted silk scaffold. **d** Hybrid scaffold seeded with BMSCs. **e** hybrid scaffold rolled up into cylindrical tendon/ligament analogues after 7 days culture of BMSCs [182]

Table 5 Electrospun polymer used in tendon/ligament tissue engineering

Polymers	Remarks	References
Silk	In vitro tenocytes culture and in vivo study of gap defect in New Zealand White rabbits' Achilles tendon showed good cell proliferation and new tissue formation	[168]
PLGA	Continuous differentiation of hMSCs into chondrogenic and osteogenic cells in PLGA nanofiber scaffold	[169]
Silk	Human MSCs adhered and grew well on the combined silk scaffolds in vitro	[170]
Silk	MSCs were distributed throughout the regenerated ligament in vivo and exhibited fibroblast morphology	[171]
Silk	MSCs-seeded scaffold was implanted in large animal (pig) model to regenerate ligament; the MSCs in regenerated ligament exhibited fibroblast morphology	[172]
PLLA	Differentiation of human tendon stem/progenitor cells (hTSPCs) was enhanced by fiber alignment	[174]
PU	Alignment of fibers affected the ECM production of human ligament fibroblast	[175]
PLDLLA	Fibroblasts seeded on crimp-like fibrous scaffolds induced increased ECM synthesis compared to those grown on scaffolds-containing uncrimped (straight) fibres	[176]
PLDLA	Fibroblasts seeded on the wavy, crimp-like fibres attached, proliferated and deposited extracellular matrix (ECM) molecules which exhibited bundle formation that resembled fascicles found in native ligament	[177]
PCL/collagen, PLLA/collagen	Heterogeneous co-electrospun scaffold mimic tendon–muscle junction	[178]
HAp/PCL, PEUUR2000	Co-electrospun-graded meshes for use ligament/bone interface	[179]
PCL	Co-electrospun scaffolds with gradients in mineral content can guide the formation of phenotypic gradients and may promote the regeneration of the L-B interface	[180]
PLGA/PLCL	PLCL microfibers were coated on PLGA-knitted structure to form a hybrid scaffold	[181]
PLGA/silk	bfGf-loaded PLGA nanofiber was coated on silk-knitted structure to form a hybrid scaffold	[173]
PLGA/silk	Sustained release of bFGF mimicked the ECM in function, stimulating mesenchymal progenitor cell (MPC) proliferation, and their tenogeneic differentiation	[182]

pulse number. hMSC adhesion and proliferation was not significantly affected by the laser ablation although their morphology varied depending on the diameter of the holes. More importantly, by using rat subcutaneous cell infiltration model, significant endothelial cell as well as M2 macrophages infiltration was observed for ablated scaffolds as cells were able to migrate through the ablated holes and infiltrate between layers of electrospun fibers into the scaffold. However, the mechanical strength was deteriorated with decreased spacing and increased hole size. Most

attempts to enhance cellular infiltration are by increasing pore size, but this unavoidably compromises the mechanical properties of the scaffolds. Alternatively, biochemical cues imparted to electrospun fibers were thought to be the solution to promote cellular infiltration into scaffold [196]. Recently, Li and co-workers [197] reported the use of hyaluronan to overcome this limitation. Hyaluronan (HA) is a highly hydrated polyanionic polysaccharide which is involved in many in vivo cellular processes and regulation of intracellular signal transduction. PCL/SF/HA fibers fabricated by emulsion electrospinning have been subjected to in vitro and in vivo tests to examine the extent of cell migration into the scaffold. The in vitro results have shown that cells can infiltrate as deep as 20–40 μm from the upper surface of HA-based scaffold. The in vivo rat subcutaneous cell infiltration model also showed penetration of cellular strands into the scaffold, while most cells were located on the surface of neat PCL scaffold. Interestingly, increased Young's modulus and elongation at break was observed with increasing HA content. This phenomenon was explained by the interaction of HA with silk fibroin (SF) that induced more β-sheet structure. This is a promising biochemical approach to solve the inherent limitation posed by dense electrospun fibers without compromising the mechanical strength of scaffold.

Another limitation of electrospinning is the scaffold thickness. During the electrospinning process, there is an electrostatic interaction between positive charged needle and negative-charged collector. Positive charge carried by polymer jet is discharged once fibers are deposited on the grounded collector. As spinning continues, fibers formed on the collector gradually become thicker, which may act as an insulator and prevent discharge and thus resulting in buildup of positive charge. The charge buildup causes the deposited fibers to repel the coming fibers. This influences the thickening of electrospun scaffold, in many reports, electrospun mats tend to be thin and are commonly several hundred micrometers thick [198, 199], which makes them nonideal for tissue engineering applications. In one recent report, self-assembled three dimensional (3D) spongiform nanofibers stacks were fabricated by conventional electrospinning through controlling experimental conditions [200]. It was found that the fibers on the top of 3D stack carried negative charge which may attract the positively charged jets during electrospinning, thus making stacking possible. Furthermore, by placing an insulating Lucite plate on the collector, a 2D thin film instead of a 3D stack is formed. It is believed that the Lucite plate blocks the discharge of fibers and as a result, electrostatic attractions are often weak and therefore the coming fibers with positive charge are repelled, which results in the formation of 2D film. Recent efforts to increase the scaffold thickness can be categorized into two types: modification of electrospinning setup and post-processing of electrospun fibers. The first involves the modification of collector to fabricate loose [201, 202] or patterned [203] 3D structure as well as putting electrostatic lens around needle tips to focus spinning jet onto the collector to increase thickness of scaffold [204]. Specifically, a water bath containing ethanol instead of an aluminum foil collector was used in wet-electrospinning to obtain a fluffy, 3D structure [202]. Electrospun fibers fabricated by such method have a thickness of 2–3 mm compared to only 40 μm from conventional electrospinning under same processing conditions. Furthermore, fiber diameters were similar for both types of fibers but porosity was significantly higher for wet-electrospun fiber. However, such loose and fluffy structures have poor mechanical strength which is another obstacle to overcome. In the post-processing of electrospun fibers, techniques such as heat-sintering [205], yarn assembly [206], and multilayered-stacking [207, 208] have been used. In an effort to increase thickness, thermally induced phase separation (TIPS) and electrospinning were combined to develop a 3D, multilayered composite scaffold [208]. Individual PCL electrospun disks were stacked into a cylindrical holder filled with PLGA solution dissolved in DMSO. It was then quenched in liquid nitrogen and DMSO was leached out. In this approach, thickness of scaffold can be increased unlimitedly by only increasing the number of stacked electrospun disks. PLGA served as effective "glue" for adhesion between individual disks. This composite scaffold exhibited similar compression strength and significantly higher tensile strength as compared to a conventional PCL scaffolds made by using TIPS. However, the pore size of the scaffold was around 5–10 μm which limits the cell infiltration. This problem may be tackled by combining this multi-layering stacking approach with some abovementioned methods to increase pore size to fabricate a 3D scaffold suitable for 3D cellular growth.

The use of harmful, volatile organic solvent in electrospinning can lead to environmental and safety problems while the toxic solvent may still remain in the electrospun fiber if proper post process treatments are not carried out [209]. For examples, 1,1,1,3,3,3-hexafluoro-2-propanol (HFIP), a volatile and corrosive solvent, which is often used in electospinning may cause severe burn and even blindness if not properly removed from the electrospun fibers. Despite their toxic and harmful nature, they are widely and commonly used in electrospinning of PLGA [210, 211], collagen [212, 213], silk fibroin [214, 215], etc. Therefore, there is a need to find replacement of such type of solvent, or even better, solvent less method to fabricate electrospun fiber. Water/alcohol/salt system [216], acetic acid [217], ethanol [218], ethanol/phosphate-buffered saline [219] have been reported for successful electrospinning of collagen [216–218] and gelatin [219]. Melt

electrospinning looks promising as it does not require the use of organic solvents, but its potential is limited by the high temperature processing and possible thermal degradation [220]. In an innovative approach, thiol-ene photopolymerization was combined with electrospinning to obtain fiber in situ in which neither solvent nor heating is required [221]. Pentaerythritol tetrakis (3-mercaptopropionate) (PETT), a tetrafunctional thiol was mixed with dipentaerythritol pentaacrylate (DPPA), an ene, along with a photoinitiator prior to electrospinning. During electrospinning, in situ polymerization of monomers occurs when triggered by exposure to UV light to furnish micro-sized fibers free of bead defects. Fibers electrospun by this thiol-ene photopolymerization present a greener approach to making fibers, e.g., no solvent, no residual, and no heat input as well as higher production rate of fiber $\sim$10 g/h compared to solution electrospinning $\sim$0.5–2.0 g/h. In another study a monomer, acrylated-epoxidized soybean oil (AESO) was used in photopolymerization to produce fibers in situ [222]. This study further confirmed the feasibility of using thiol-ene chemistry in making fibers. However, this novel technique, in situ photopolymerization requires careful manipulation of parameters, for instance, photocuring time, molar ratio of thiol-ene groups, position of UV light source, and viscosity. Furthermore, choice of monomer is limited and the fibers formed may not be biocompatible which makes it unsuitable for biomedical application.

Drug delivery

The goal of designing a drug delivery system is to enable the release of drug at a controlled rate over a desired period [223]. Electrospinning has also found application in the field of drug delivery due to its ability to fabricate nanofibers that can act as a drug carrier because of their good functional characteristics such as high surface area, which is associated with better dissolution rate, ease of incorporation of drug, and limited time for drug recrystallisation resulting from faster solvent evaporation [224]. Besides this, various biomolecules have been successfully incorporated into electrospun nanofibers for controlled release, e.g., gene [225], proteins [47, 226, 227], and enzymes [32]. In terms of processing setup, there are two approaches in incorporating biomolecules in fibers: blend electrospinning and coaxial electrospinning [228]. In blend electrospinning, the polymer and biomolecules are mixed prior to electrospinning whereas in coaxial electrospinning, both polymer and biomolecules are coaxially and simultaneously electrospun to produce fibers with a core–shell structure. Saraf and co-workers [225] constructed fiber mesh scaffolds by coaxial electrospinning and encapsulated plasmid DNA within the core and a nonviral gene delivery vector within the sheath of the fibers. The release of the gene delivery vector was studied over 60 days during which the vector release was controlled by changing the parameters such as the concentration of the plasmid DNA. In addition, transfection efficiency of the plasmid DNA was varied by changing the concentration and molecular weight of the core polymer. The release profile and transfection properties could be fine-tuned by changing the processing parameters. In another study, PCL-based nanofibrous scaffold was incorporated with bovine serum albumin (BSA). The loaded protein was distributed homogeneously within the core of the fibers and better sustained release profiles were exhibited by scaffolds made from coaxial electrospinning. PEG helped to preserve up to 75 % of the initial biological activity of the protein in the coaxial electrospun scaffolds [226]. Coaxial electrospinning is more favorable in the fabrication of scaffolds for use in drug delivery as the release of growth factors is better controlled for core–shell nanofibers than that of the blended nanofibers. The burst release of 43.8–48.5 % loaded proteins observed within the first 6 h for the blended nanofibers was reduced to 17.4–18.9 % in coaxial electrospun nanofibers followed by stable and sustained release [47]. Cross-linking may help to prevent burst release of drug from nanofibers. Crosslinked PLGA/gelatin nanofibers showed depressed burst release of the drug fenbufen at the initial release stage [227]. Cross-linking of PVA nanofibers also resulted in better enzyme release profile, due to the water resistant property of the cross-linked PVA fibers, thereby making it an effective diffusive barrier for regulating the enzyme release in reaction medium [32].

Many drug delivery systems are specifically designed for targeted application such as oral-drug delivery, colon-targeted drug delivery, fast-dissolving drug delivery, sequential chemotherapy, and even the prevention of HIV transmission. A linear delivery system of nifedipine was designed using a simple fabrication method for oral drug delivery. The tablet capped with thinner sheets exhibited a burst release at an early stage whereas the tablet capped with thicker sheets controlled the drug release at the late stage (Fig. 9a). The correct combination of two different tablets (Fig. 9c) was expected to give a linear drug release profile. Combination of two tablets capped with PLGA nanofibrous membrane of thickness 50 and 75 μm, respectively, showed a linear drug release profile ($R^2 > 0.983$) independent of pH with 100 % of drug released within 24 h (Fig. 9b), which is desirable for oral drug delivery [229]. Diclofenac sodium, a nonsteroidal antiinflammatory drug, was incorporated into Eudragit® L 100-55, a pharmaceutical excipient that has been used in colon-targeted drug delivery and electrospun into nanofibers. The drug release profile of the electrospun nanofibers was dependent on pH and the nanofibers exhibited better

sustained drug release profile than that of a physical mixture of diclofenac sodium and Eudragit® L 100-55 [230]. Electrospun Polyvinylpyrrolidone (PVP) nanofibers have great potential in improving the dissolution of poorly water soluble drugs due to the high solubility of PVP, high specific surface area of the nanofibers and good drug dispersal in the nanofibers [231].

Combination therapy such as sequential chemotherapy requires sustained release of multiple drugs so that the release order, timing and dose must be controlled. A tetra-layered PLCL nanofibers mesh was designed to examine the efficiency of the multilayered system in sustained release of two different drugs independently. The four layers of the mesh were (i) chromazurol B-loaded mesh, (ii) barrier mesh, (iii) 5,10,15,20-tetraphenyl-21*H*,23*H*-porphinetetrasulfonic acid disulfuric acid-loaded mesh, and (iv) basement mesh. The PLCL nanofiber diameter affected the speed of drug release while the mesh thickness influenced the duration of sustained release. The desired release profile of the dual drug could be achieved by fine-tuning the process parameters that affect the morphological features of the tetra-layered nanofibers, thus finding use in sequential therapy system [232].

Cellulose acetate phthalate (CAP) fibers were incorporated with antiviral drugs to prevent man-to-woman HIV transmission. The prevention was made possible as the electrospun CAP fibers are not soluble in healthy vaginal fluid, which has a pH of below 4.5, but are soluble in small amounts of human semen having pH between 7.4 and 8.4. CAP fibers are nontoxic to vaginal epithelial cells at concentration below 2 mg/ml and did not impede the proliferation of the vaginal microbial flora. Moreover, CAP fibers without antiHIV drugs also inhibited the HIV infection of CD4+ TZMbl cells in vitro. However, further in vivo studies are needed to explore the potential of CAP fibers in preventing HIV transmission during sexual intercourse [233]. Table 6 contains a list of polymers and techniques used to load drug molecules into fiber for biomedical applications.

Although electrospun fibers serve as excellent drug carriers, there are still some limitations or issues that need to be addressed. Initial burst release of drug from fibers has

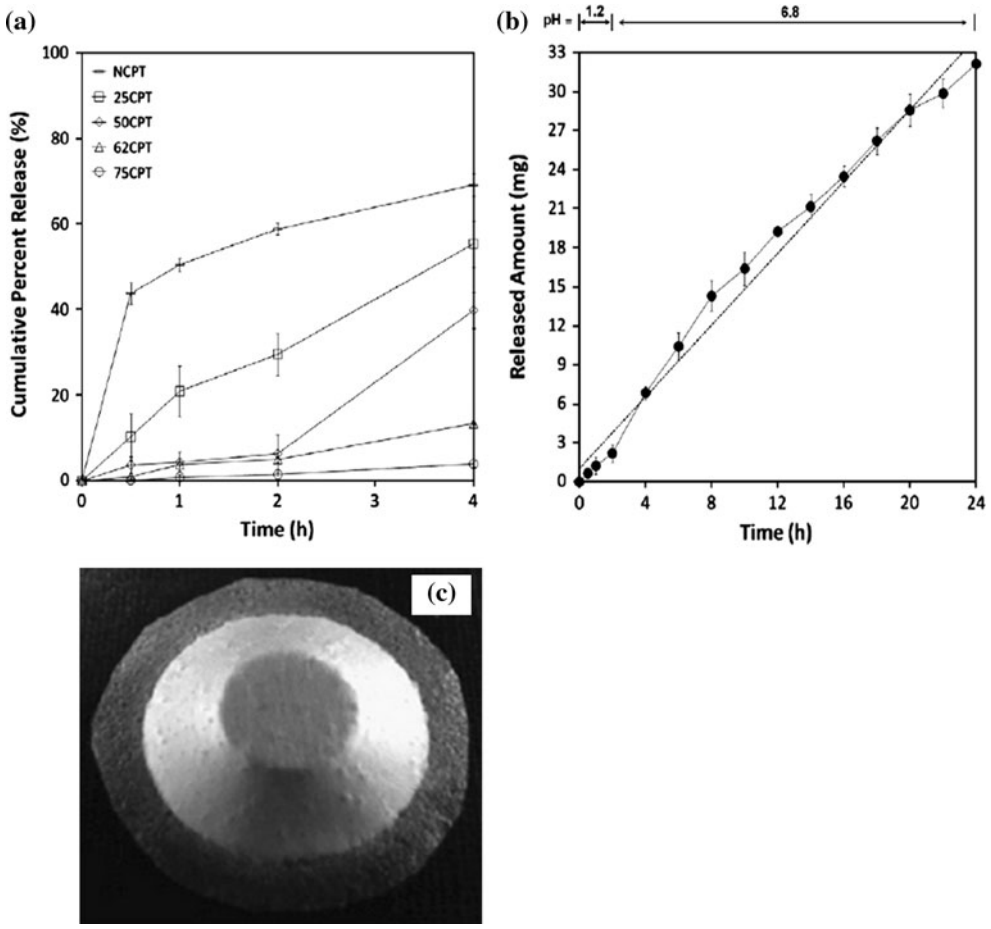

Fig. 9 **a** Release profile of nifedipine from capped tablets of different thickness at pH 6.8. **b** Release profile of nifedipine from a combination of two capped tablets, 50 and 75CPT). **c** Macroscopic image of 25 CPT *(*NCPT* noncapped tablet, *25CPT* capped tablet with nanofiber of thickness 25 μm) [229]

Table 6 Electrospinning techniques used in drug delivery system

Polymers	Technique used	Molecules loaded/application	References
Poly(ethylenimine)	Coaxial electrospinning	Plasmid DNA	[225]
PLLACL/collagen	Coaxial/blend electrospinning	Protein (bone morphogenetic protein 2 and dexamethasone)	[131]
PCL	Coaxial/blend electrospinning	Protein (bovine serum albumin)	[226]
PLGA/gelatin	Blend electrospinning	Protein (Fenbufen)	[227]
PVA	Coaxial electrospinning	Enzyme (lactate dehydrogenase)	[32]
PLGA	Tablet capped with electrospun fiber	Oral drug delivery	[229]
		Colon-targeted drug delivery	[230]
PVP	Blend electrospinning	Fast dissolving drug delivery	[231]
PLCL	Sequential electrospinning	Tetralayered nanofibers in controlling release of multiple drugs	[232]
CAP	Blend electrospinning	Prevention of HIV transmission	[233]
PLGA	Blend electrospinning	Local anesthetic, bupivacaine	[234]
PCL	Blend electrospinning	Air-controlled drug delivery by using super hydrophobic polymer dopant	[235]
PCL	Blend electrospinning	Air-controlled drug delivery to release anticancer drugs	[236]
PLLA	Dual spinneret electrospinning	Dual drug delivery	[237]
PAM14	Blend electrospinning	Multicomponent, bioerodible polymeric delivery system	[238]
PVA	Blend electrospinning	Dye-loaded PLGA nanoparticles encapsulated into nanofibers	[239]
PLLA	Blend electrospinning	Dual drugs-loaded chitosan microspheres encapsulated into nanofibers	[240]
PLLA	Emulsion electrospinning	Entrapped Ca-alginate as reservoirs for drugs in fibers	[241]
PVA	Blend electrospinning	Antibacterial microemulsion containing eugenol/PVA composite	[242]
PLLACL	Emulsion electrospinning	Dual release of rhodamine B and bovine serum albumin (BSA)	[243]
PEG-PLA	Emulsion electrospinning	Dual release of paclitaxel (PTX) and doxorubicin hydrochloride (DOX),	[244]
PDLLA	Emulsion electrospinning	Delivery of BSA	[245]
PLGA	Dripping or Blend Electrospinning	DNA-loaded chitosan nanoparticles-coated outside or within fibers	[246]
PCL	Coaxial or blend electrospinning	Enzyme-loaded liposome embedded in fibers	[247]

long been one of the main problems encountered by the researchers especially when the drug loading is higher, probably due to the aggregation of drug molecules near the surface of fibers [234]. This always happens when the drugs are directly encapsulated into or mixed with polymer solution prior to electrospinning. Recently, it was suggested that the use of superhydrophobic polymeric agent may help to slow the burst release at early stage and prolong the sustained release of drug [235]. PCL electrospun meshes containing 0–50 wt% poly(glycerol monostearate-*co*-ε-caprolactone) (PGC-C18), which acts as hydrophobic dopant was fabricated followed by loading it with a model bioactive agent, SN-38 (7-ethyl-10-hydroxycampthothecin). The entrapment of air layer within the electrospun meshes prevented the penetration of water into the meshes and retarded the hydrolysis of polymer and thus the release of drug. The authors were able to demonstrate that the rate of water penetration and displacement of entrapped air were related to the apparent contact angle of the meshes, e.g., its extent of hydrophobicity. PCL electrospun meshes doped with 10 wt% PGC-C18 showed near to linear sustained release over 70 days whereas pure PCL electrospun meshes showed relative fast drug release for the first 10 days and reached maximum cumulative release of about 70 % after 20 days. As expected, PCL meshes doped with even higher content of the hydrophobic dopant (30 and 50 wt%) exhibited only ~10 % release over 9 weeks. In their expanded work, a more medium-soluble drug, Campthothecin-11 (CPT-11) was incorporated into PCL electrospun meshes [236]. Without PGC-C18, the meshes released CPT-11 very quickly and reached 60 % over a few days whereas 10 wt% of PGC C18-reduced dramatically the CPT-11 release to a similar cumulative release only after about 40 days. The delay of drug release by the hydrophobic meshes is through the reduced drug diffusion and increased stability of the entrapped air layer. Furthermore, the mesh location and drug release was monitored by ultrasound, which also confirmed that the trapped air was responsible for the slow sustained drug release. However, the drug distribution within the PCL fibers was not homogenous, which is the common problem in direct encapsulation of drug into fibers. For example,

higher drug concentration was seen at the center of fibers for 1 wt% SN-38 whereas higher drug concentration was seen partitioned to the surface for 0.1 wt% SN-38 [236].

Apart from nonhomogeneity of drug distribution within fibers, the direct encapsulation of drug affects adversely the mechanical property, e.g., the tensile strength of electrospun PLGA suture was found to decrease with increasing drug content [234]. Besides this, some applications require the use of multiple drugs, but the presence of two drugs in the same polymer matrix has been shown to interfere with the release kinetics of at least one of the drugs [237] and caused heterogeneous distribution of the other drug [238]. Therefore, investigation on the use of particle/polymer electrospun composite in drug delivery is fast becoming popular [239, 240]. The composite can be prepared through emulsion electrospinning [241, 242] and separate preparation of nanoparticle or microsphere [235, 236, 239, 240]. Researchers have now shifted their interest from loading single drug to dual drugs, especially one hydrophobic and another one hydrophilic [243, 244]. Yohe et al. [235] loaded mesoporous silica nanoparticles (MSNs) with hydrophobic drug rhodamine B (RHB) before electrospinning them together with PLGA containing another hydrophilic drug, fluorescein (FLU). The advantages of such kind of composite are: (1) the MSNs spheres are distributed homogeneously within the composite fibers; (2) no interaction of drugs (RHB & FLU); (3) no initial burst effect of drug (RHB) loaded in MSN; these problems are frequently encountered when the drugs are directly incorporated into the fibers. However, due to higher hydrophilicity and direct encapsulation, most of the FLU released rapidly after 324 h. For this reason, in another reported work the authors loaded both drugs, RHB and FLU separately into MSNs spheres [236]. The results were encouraging, FLU showed a prolonged release: the cumulative release percentage depended on the weight ratio of the two drugs as well as the initial concentration of PLGA. These studies have successfully demonstrated that such composite system can promote sustained and independent release of dual drugs.

Another challenge faced by researchers in the field of drug delivery is to ensure the bioactivity or functional efficiency of drugs are not affected adversely during the fabrication process or due to the delivery design. Ultrasonication during polymer preparation and high voltage during electrospinning process could alter protein structure to some extent [245]; DNA loaded into chitosan particles within or attached outside fiber have relatively high transfection efficiency compared to the naked one [246]. In a recently published study, researchers proposed the combined use of liposome and fibers as drug delivery system [247]. Core/shell nanofibers containing intact liposomes were successfully fabricated by using coaxial electrospinning. To investigate the protective effect of liposomes on bioactivity, in this case enzymatic activity of drug, a protein, horseradish peroxidase (HRP) was used. Four types of designs were shown: B-HRP, B-LIP, K-HRP, K-LIP. The first two were fabricated by blend-electrospinning in which B-HRP refers to HRP blend with PVA and B-LIP refers to HRP loaded into liposome. K-HRP and K-LIP were also similar with the first two, except they were made by using coaxial-electrospinning. PVA was used as both core and shell polymer. The enzymatic activity tests showed that both co-electrospun fibers, with (K-LIP), or without (K-HRP) liposomes exhibited significantly higher enzymatic activity than the blend electrospun fibers. This again confirmed the inferiority of direct encapsulation of drug molecules into fibers in terms of retention of drug's bioactivity, with many other disadvantages mentioned above. More importantly, the results also showed that K-LIP has much higher enzymatic activity than K-HRP, demonstrating that liposome has the ability to preserve the enzymatic activity of the protein, HRP. This opens a new perspective for researcher to consider the use of liposome in future drug delivery research.

Wound dressing

The ultimate purpose of a wound dressing is to achieve the fastest rate of healing and the best aesthetic repair of the wound [248]. Fibers fabricated by electrospinning are excellent candidate for wound dressing because they can absorb wound exudates more efficiently, prevent drying up of the wound, protect the wound from bacterial infection, allow gas permeation and have good conformability [248]. Furthermore, various polymeric materials [249, 250] can be used for dressing manufacturing and easy incorporation of bioactive molecule/agent to provide extra functions such as antiinflammatory activity [251] and promote tissue growth [252]. These excellent characteristics are due to the high surface area to volume ratio, porosity, electrospinnability from hydrophilic polymer and drug-loading capacity of the fibers. A list of different polymers, solvents, and approaches taken to enhance the functionality of skin graft is presented in Table 7.

In vitro studies indicated that PLGA/collagen nanofibers can be used as accelerators for wound healing in the early stage [249]. The combination of PCL and gelatin was explored where the composite was electrospun directly onto a commercially available polyurethane dressing (Tegaderm^{TM}, 3M Medical) [250]. *Calendula officinalis*, a wound-healing and antiinflammatory agent was mixed with hyperbranched polyglycerol and electrospun into nanofibers. The morphology and mechanical properties of the nanofibers such as tensile modulus and elongation-to-break value were influenced by the concentration of *C. officinalis*. In vivo histocompatibility test on female rats showed good

Table 7 Different approaches in wound dressing

Polymers	Solvents	Remarks	References
PLGA/collagen	HFIP (hexafluoroisopropanol)	Effective wound-healing accelerators in early stage wound healing	[249]
PCL/gelatin	TFE (2,2,2-trifluoroethanol)	Nanofibers scaffold electrospun on a polyurethane dressing	[250]
Polyglycerol	Methanol/DMF	Nanofibers-contained *Calendula officinalis* as wound healing and antiinflammatory agent	[251]
Silk	Aqueous solution with 5wt % PEO	Silk fibers-contained epidermal growth factor (EGF) for skin regeneration	[252]
Cellulose, cellulose/chitosan, cellulose/PMMA	DMSO, DMF	Cell lytic enzyme, lysostaphin (Lst) was immobilized on cellulose-based fibers	[253]
N-Carboxyethylchitosan/PEO	Formic acid	Hybrid nanofibrous yarn incorporated with silver nanoparticles to give antibacterial activity	[256]
SiO_2		Reusable wound covered with antibacterial silver nanoparticles	[36]
Soldium alginate/PVA	Distilled water	Fibers incorporated with nano-ZnO exhibited antibacterial activity	[258]
PLGA	DCM	Study of interaction of antibacterial PLGA with biochemical wound environment	[259, 260]
PU	DMF/THF	Dextran/polyurethane (PU) carrying ciprofloxacin HCl (CipHCl) drug	[261]
PU	DMF/THF	Cellulose acetate/PU containing polyhexamethylene biguanide as antimicrobial agent	[262]
PLGA	DMF/chloroform	Hybrid and core/shell chitosan/PLGA made by coelectrospinning and coaxial electrospinning	[264]
PVA	DI water	Chitosan coated PVA for wound dressing	[265]
PVA, PCL, etc.	Water, DMF, chloroform, etc.	Comparison of various polymers on in vivo wound healing performance	[266]
PCL	Chloroform/methanol	Four types of plants extract incorporated separately into fiber	[267]
EVOH	Propan-2-ol	Poly(ethylene-*co*-vinyl alcohol) (EVOH) nanofibers encapsulated with Ag nanoparticles	[268]
Polyurethane	DMF	Polyurethane nanofibers encapsulated with Ag nanopaticles	[269]
Silk fibroin	Formic acid	Silk fibroin nanofibers encapsulated with TiO_2 nanoparticles	[270]
PDLA/PLLA	Chloroform	Polylactide stereocomplex-based fiber with antibacterial and hemostatic properties without using particle and bioactive agents	[274]
Cellulose acetate	Acetone, DMAc	Antioxidant cellulose acetate fiber mats containing asiaticoside or curcumin	[279]
PCL/gelatin	THF/DMF, acetic acid	Application of needleless electrospinning in wound healing	[286]

integration between the nanofibers and the host tissue, with collagenous connective tissue regeneration and re-epithelialization on the 2nd day after surgery [251]. Besides an antiinflammatory agent, nanofibers have been functionalized with lytic enzyme as well as epidermal growth factors (EGFs). A novel antimicrobial therapy was developed to combat "super bacteria" that are resistant to any antibiotics [253]. Inspired by the behavior of bacteria that use cell lytic enzymes to eliminate other bacteria, the researchers immobilized lysostaphin (LSt), a cell lytic enzyme, onto cellulose-based nanofibers. Cellulose, cellulose–chitosan, and cellulose PMMA were functionalized with lysostaphin through oxidation, cross-linking and hydrolysis, respectively. Both oxidized and hydrolyzed cellulose-based nanofibers showed complete neutralization of activity of *Staphylococcus aureus* in antimicrobial assay. By using a keratinocyte-based in vitro test, (Fig. 10a), it was found that the oxidized cellulose fibers embedded with lysostaphin completely damaged the *S. aureus* cells, which demonstrates that the oxidized cellulose nanofibers functionalized with cell lytic enzyme have potential to combat super bugs such as methicillin-resistant *S. aureus*. Either in free solution or in contact with cellulose-based nanofibers, the presence of lysostaphin killed all *S. aureus* cells (Fig. 10b, c). In additionally, such type of nanofibers mats-revealed minimal cytotoxicity toward keratinocytes (HaCaT cell lines), indicating their biocompatibility. Furthermore, EGF was incorporated into a silk nanofibrous mat to investigate its possible use to accelerate the re-epithelialization during the wound healing process [252].

The observed initial burst release of EGF is considered favorable because it helps to rapidly activate the keratinocytes. An in vitro 3D model of human skin was used to investigate the efficiency of the nanofibers in wound closure. The nanofibrous silk mat containing EGF greatly accelerated the wound closure compared to the nanofibrous silk mat without EGF.

Silver nanoparticles are well known for their antibacterial activity against a wide range of pathogenic microorganisms and as a result have found application in wound-healing [254, 255]. Various ways have been reported to incorporate silver nanoparticles into polymic fibers. In one study, silver nitrate was dissolved with the polymer-spinning solution, which also acted as a reducing agent, followed by electrospinning. The TEM results indicated that the presence of silver nitrate in the spinning solution influenced the morphology of the fibers. Electrospun carboxyethylchitosan/PEO fibers containing 0.02 M silver nitrate exhibited a smooth surface and cylindrical shape whereas fibers containing 0.04 M of silver nitrate showed extremely fine dendrite-like structures. The formation of dendrite-like structures was attributed to ionic imbalance caused by the low molecular weight of silver nitrate salt on the surface of the charged polymer jet during the electrospinning process [256]. However, the loading of silver nanoparticles directly into nanofibers may negatively influence the antibacterial performance because antibacterial activity of silver nanoparticles is the result of direct contact of silver with bacteria. Therefore, in another study, silver nanoparticles were grafted onto SiO_2 nanofibers after the electrospinning process by dispersing the silica in aqueous silver nitrate solution of different concentration followed by heating for different times. It was reported that the density of silver nanoparticles on the surface of fibers can be controlled by the concentration of silver nitrate solution, incubation temperature and time. The nanoparticle size was slightly increased with increasing concentration but significantly reduced by increasing incubation temperature [257]. Apart from silver nanoparticles, the incorporation of zinc oxide nanoparticles into sodium/alginate composite nanofibers also exhibited antibacterial activity. However, higher
cytotoxicity with higher ZnO concentration revealed a need to identify an optimal concentration that minimizes the toxicity while maximizing the antibacterial activity [258].

An aspect in wound healing which is not fully explored is the dynamic interactions of nanofibrous mats with the environment of the wound. The participation of PLGA electrospun ultrafine fibers in a dynamic interaction with three bacterial strains was studied. The formation of a

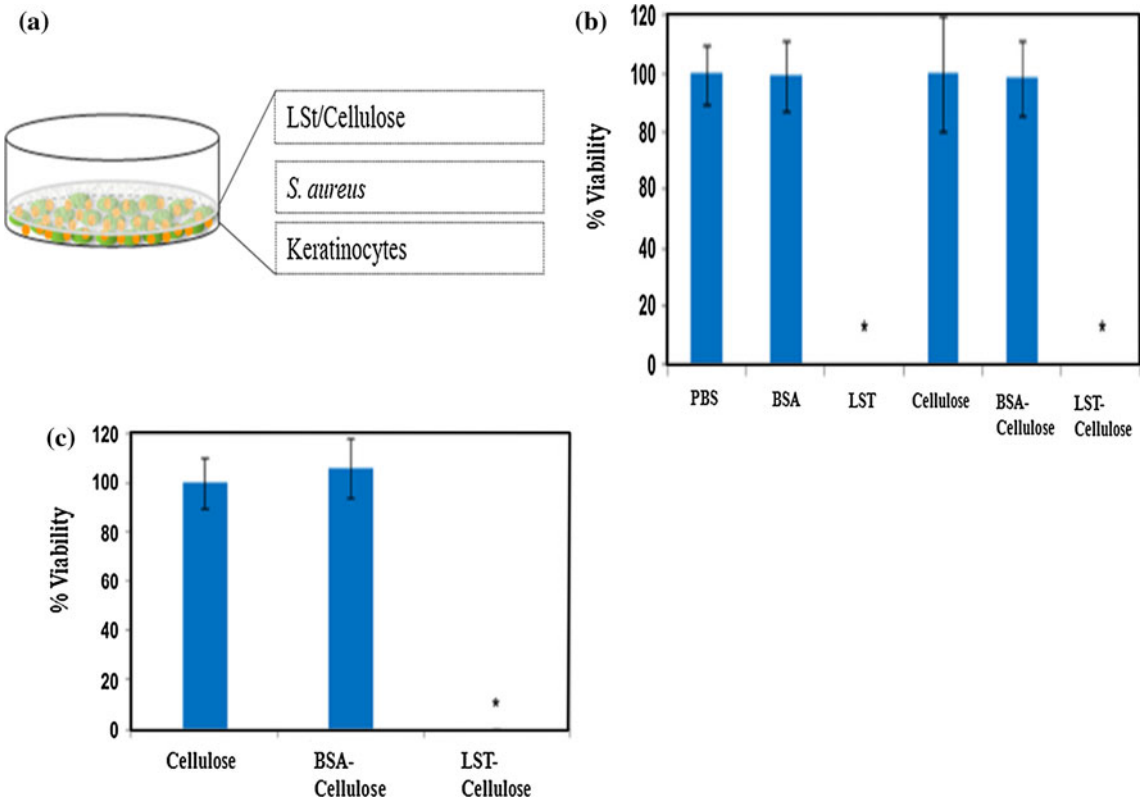

Fig. 10 **a** Skin model composed of keratinocytes, *S. aureus* suspension and cellulose nanofibrous mats functionalized with LSt. **b** % Viability of *S. aureus* cells in free solution. **c** % Viability of *S. aureus* cells on cellulose-based nanofibers [253]

dense biofilm of bacterial colonization was evident when the PLGA fibers were exposed to wound bacteria for 24 h, suggesting that the PLGA fiber acted as a good template for bacterial growth. Interestingly, the presence of bacterial stacks enhanced the drug release, which damaged the fibers and decreased the pH. The faster drug release eliminated the planktonic bacteria and suppressed the biofilm [259]. The potential response of the fusidic acid (FA)-loaded ultrafibers to control microbial bioburden was further studied to understand the mechanism of this phenomenon. The results revealed a significant increase in initial drug release even at low bioburden level (10^3 CFU/ml), which could be due to the hydrolysis induced by bacterial enzymes resulting in degradation and erosion of the FA-loaded PLGA ultrafine fibers, thus resulting in faster FA release [260].

Synthetic hydrophobic polymers such as polyurethane (PU) [261, 262], PLA [263], PCL [250], and PLGA [264] are ideal candidates in wound dressing due to their good mechanical properties. However, their hydrophobic nature renders them low affinity toward water, which fails to preserve aqueous and moist environment required by wound healing process. Therefore, natural hydrophilic polymer such as dextran [261], chitosan [263, 265], cellulose acetate [262], gelatin [250], and collagen [249] are always used to blend with those hydrophobic polymers for use in wound dressing because hydrophilicity is essential to accelerate wound healing [266]. In vitro and in vivo evaluation of these composite electrospun fibers has confirmed their potential in the field of wound dressing. Nevertheless, the mechanical aspect of wound dressing candidates has always been overlooked. For practical use, the elastic modulus (or Young's modulus), which indicates the hardness, must be high enough so that dressing will not break easily during the healing process but the mechanical properties of the dressing will change after interacting with aqueous environment surrounding the wound. For example, the Young's modulus of the core/shell PLGA/chitosan membrane decreased dramatically from 178.7 ± 50.4 MPa in dry state to only 2.42 ± 0.54 MPa in the wet state [264]. It falls far outside the range of the tensile modulus of human skin which is between 15 and150 MPa [267]. Further, a study done by Liu et al. [266] showed that conventional cotton gauze-possessed tensile strength of 11.1 MPa which is significantly higher than polymer such as PVA (3.67 MPa), PAN (1.22 MPa), PCL (4.11 MPa), PAN–PU (6.64 MPa), and so forth. The incorporation of hydrophilic polymer would even lower their tensile strength. However, it should be noted that since wound dressing is seldomly under a high tensile strength at the wound site and is not likely to be used in high load-bearing locations, the maximum tensile strength should not be as important as the elastic modulus [267]. Therefore, it is imperative that researchers report the tensile modulus of wound dressing before use as well as that in the wet state during in vivo healing process, especially when hydrophilic polymers are used.

Another concern has been the safety issue of nanoparticles such as silver [268, 269] and titania [270] in wound dressing when used for their antibacterial properties. Specifically, silver nanoparticles at only 5–50 μg/ml have been shown to exhibit toxicity towards rat liver cells. Decreased mitochondrial function, increased reactive oxygen species (ROS) and reduced glutathione (GSH) levels were observed in the liver cells [271]. It is believed that due to small size nanoparticles can be easily adsorbed into biological tissues through inhalation, injection, and taken up by body organs and tissues. They may interact with cell mitochondria, thus induce major structural damage and cause DNA mutation [272]. Nevertheless, there is evidence that the reduction from micro- to nano-size does not necessarily translate to toxicity [273]. This debatable topic is still ongoing in the toxicology research community. Therefore, it would be better to take another approach which can fulfill the antibacterial requirement in wound dressing. Without adding any antibacterial agent, an antibacterial novel fibrous mesh was electrospun from the solution of poly(D- or L-)lactide and diblock copolymers consisting of poly(L- or D-)lactide and poly(*N,N*-dimethylamino-2-ethyl methacrylate) blocks. The antibacterial as well as hemostatic properties were imparted by the tertiary amino groups from the poly(*N,N*-dimethylamino-2-ethyl methacrylate) blocks [274]. Plant extracts have long history of being used in the treatment of burn and wound healing, especially in India and China [275]. Extract from plants such as *Ixora coccinea* [276], *Dendrophthoe falcate* [277], *Bridelia ferruginea* [278] and many more have shown good antibacterial as well as wound healing properties. The fact that they have been used in traditional medicine for so long have proved that these plant extracts are more or less safe to humans and they are being continuously studied by natural product researchers using in vitro or in vivo test until now. Recently, Jin et al. [267] have successfully electrospun four different plant extracts, namely *Indigofera aspalathoides, Azadirachta indica, Memecylon edule* and *Myristica andamanica* along with PCL. Interestingly, the incorporation of these plant extracts increased the hydrophilicity of PCL, otherwise it is generally not suitable to be used as wound dressing material due to its inherent high hydrophobicity. In vitro test indicated that the fibers electrospun with *Memecylon edule* showed the greatest potential to be used in skin graft. Similarly, in an earlier study asiaticoside and curcumin from plant extract were electrospun along with fibers [279]. The as-loaded herbal substances were stable up to 4 months of storage, either at room temperature or 40 °C. Furthermore, the antioxidant

activity of curcumin was retained after loading into fibers. In short, it is obvious that plant extracts can be combined with electrospinning technique to impart fibers with desirable properties in wound dressing without serious safety issue.

From a practical point of view, electrospun wound dressing is difficult to be produced on an industrial scale due to the low flow rate (1–5 ml/h) used in the fabrication process. The effort of solving this limitation was not significant until 2004 when Yarin and Zussman [280] introduced the use of needleless electrospinning. The needleless electrospinning differs from the original electrospinning technique in which many Taylor cones can be formed and multiple electrified jets are stretched into fibers simultaneously to dramatically increase the production rate. One added advantage is that since no needle is used, this new technique has avoided the problem of clogging. Since then, more preliminary studies have been devoted to modify and improve the needleless electrospinning unit, mostly on the geometry of spinneret [281–285]. Recently, gelatin and PCL nanofibers were prepared using needleless electrospinning [286]. In vitro results using human dermal fibroblasts, kerationcytes and mesenchymal stem cells showed that both nanofibers-promoted cell attachment and growth whereas in vivo results in rat showed improvement of wound closure was observed for gelatin but not for PCL. In fact, such results were expected because unlike gelatin, PCL is hydrophobic and not suitable to be used alone as wound dressing. Nevertheless, this study demonstrated the feasibility of using needleless electrospinning in the area of wound dressing. Needleless electrospinning, which is still in its infancy, warrants further investigation from biomedical engineering community.

Concluding remarks and future perspectives

Electrospinning, an "old" technique that has been used to fabricate fibers, did not gain popularity until researchers gained a sufficient understanding of its processing parameters in order to exploit its full potential in various applications. The main advantages of electrospinning are the ability to produce continuous nanoscale fibers, high surface area-to-volume ratio, functionalizability of surface of fibers, simplicity of the electrospinning process and the possibility of industrial mass production. The properties of electrospun nanofibers can be easily modified by controlling the electrospinning process, for example, the use of rotating collector results in aligned fibers, which is favorable for tissue engineering applications. Past research has shown that a wide range of polymers, either natural or synthetic, can be electrospun into nanofibers. Ceramics such as bioactive glass have received increasing research attention because of their good biocompatibility, either electrospun into nanofibers or incorporated with a polymer to produce a composite. Electrospinning has attracted many uses in biomedical application such as tissue engineering, drug delivery, and wound dressing. Optimization of electrospinning process parameters has been emphasized in most publications to cater for the needs of biomedical applications such as aligned fibers for use in nerve engineering. The possibility of incorporating bioactive agents or functional nanoparticles broadens the use of electrospinning in wound dressing applications. Some researchers have attempted to solve issues such as limited infiltration of cells resulting from small pore size, the initial burst release in drug delivery system by designing new electrospinning processes such as co-axial electrospinning, sequential electrospinning, and combining electrospinning with other techniques. This is essentially important, because most research in electrospinning looks promising but without solving critical and basic inherent limitations such as too small pore-size, scaffold too thin due to dense fibers, it cannot be brought into clinical level. It is hoped that more efforts in future will address these issues.

Although electrospinning has been boasted as a technique of choice to fabricate scaffold for tissue engineering, the 3D structures made so far are either fluffy, in a loosened packing or multilayered packing that offers too small pore size, which inhibits cellular infiltration and scaffolds suffer from inferior mechanical properties. It is very difficult to solve this inherent limitation of electrospinning by manipulation of process parameters, however, the solution to the problem may lie in the combined use of electrospinning with other technique such as rapid prototyping. Rapid prototyping is a well known versatile 3D-strucutre making technique which uses computer-aided design (CAD) data. The shortcoming of rapid prototyping is that this technique creates pores which are too large for cell seeding and it cannot create nanoscale features that mimic ECM which are essentially the strengths of electrospinning. These complementary techniques may help researchers to fabricate a true 3D structure that fulfills the cellular and mechanical requirements of biomedical scaffold in tissue engineering.

Despite the versatility of electrospinning in spinning a variety of materials to be used in biomedical applications, the main issue will be to bring the promising research into industrial level. Given its low production rate, there is still a long way to take this technique to production level. Although, technique such as needleless electrospinning technique has been developed recently to tackle this widely recognized issue but it is still in its infancy. Moreover, process variables to control fiber morphology, functionality and applicability in applications in the new technique are yet to be studied. To summarize, the technique of

electrospinning warrants further research and its use and real importance in the field of biomedical applications will be realized when the electrospun fibers enter into the clinical level and are produced at large scale.

Acknowledgements The authors acknowledge the financial support from MyPhD Scholarship (880330235485) from the Ministry of Higher Education, Malaysia.

References

1. Rayleigh L (1882) Philos Mag 14:184
2. Formhals A (1934) US Patent 1975504
3. Simons HL (1966) US Patent 3280229
4. Taylor G (1969) Proc R Soc Lond Ser A Math Phys Sci 313(1515):453
5. Peter KB (1971) J Colloid Interf Sci 36(1):71
6. Annis D, Bornat A, Edwards RO, Higham A, Loveday B, Wilson J (1978) Southern Med J 71(1):209
7. Larrondo L, St. John Manley R (1981) J Polym Sci 19(6):921. doi:10.1002/pol.1981.180190602
8. Fisher ACDCL, How TV, Annis D (1985) Life Support Syst 1:462
9. Reneker D, Chun I (1996) Nanotechnology 7(3):216
10. Sill TJ, von Recum HA (2008) Biomaterials 29(13):1989
11. Frenot A, Chronakis IS (2003) Curr Opin Colloid In 8(1):64
12. Kumbar SG et al (2008) Biomed Mater 3(3):034002
13. Barnes C, Sell S, Boland E, Simpson D, Bowlin G (2007) Adv Drug Deliv Rev 59(14):1413
14. Charernsriwilaiwat N, Opanasopit P, Rojanarata T, Ngawhirunpat T, Supaphol P (2010) Carbohyd Polym 81(3):675
15. Beachley V, Wen X (2009) Mat Sci Eng: C 29(3):663
16. Sencadas V, Correia DM, Areias A, Botelho G, Fonseca AM, Neves IC, Gomez Ribelles JL, Lanceros Mendez S (2011) Carbohyd Polym 87(2):1295
17. Tan SH, Inai R, Kotaki M, Ramakrishna S (2005) Polymer 46(16):6128
18. Pakravan M, Heuzey M-C, Ajji A (2011) Polymer 52(21):4813
19. Van der Schueren L, De Schoenmaker B, Kalaoglu ÖI, De Clerck K (2011) Eur Polym J 47(6):1256
20. Yang F, Murugan R, Ramakrishna S, Wang X, Ma YX, Wang S (2004) Biomaterials 25(10):1891
21. Hartgerink JD, Beniash E, Stupp SI (2001) Science 294(5547):1684
22. Yu J, Qiu Y, Zha X, Yu M, Yu J, Rafique J, Yin J (2008) Eur Polym J 44(9):2838
23. Zhang Y, Li J, Li Q, Zhu L, Liu X, Zhong X, Meng J, Cao X (2007) J Colloid Interf Sci 307(2):567
24. Nirmala R, Kalpana D, Jeong JW, Oh HJ, Lee J-H, Navamathavan R, Lee YS, Kim HY (2011) Colloids Surface A 384(1–3):605
25. Cao H, Chen X, Yao J, Shao Z (2012) J Mater Sci pp 1–6. doi: 10.1007/s10853-012-6722-6
26. Zhang W, Li H-P, Pan W (2012) J Mater Sci pp 1–7. doi: 10.1007/s10853-012-6717-3
27. Shabani I, Hasani-Sadrabadi MM, Haddadi-Asl V, Soleimani M (2011) J Membrane Sci 368(1–2):233
28. Nair AS, Jose R, Shengyuan Y, Ramakrishna S (2011) J Colloid Interf Sci 353(1):39
29. Wang L, Yu Y, Chen PC, Zhang DW, Chen CH (2008) J Power Sources 183(2):717
30. Zhang H, Zhao Q, Zhou S, Liu N, Wang X, Li J, Wang F (2011) J Power Sources 196(23):10484
31. Zheng Y, Wang J, Yao P (2011) Sensor Actuat B: Chem 156(2):723
32. Moreno I, González-González V, Romero-García J (2011) Eur Polym J 47(6):1264
33. Shao S, Li L, Yang G, Li J, Luo C, Gong T, Zhou S (2011) Int J Pharm 421(2):310
34. Soletti L, Nieponice A, Hong Y, Ye S-H, Stankus JJ, Wagner WR, Vorp DA (2011) J Biomed Mat Res-A 96A(2):436
35. Wang C-Y, Zhang K-H, Fan C-Y, Mo X-M, Ruan H-J, Li F–F (2011) Acta Biomater 7(2):634
36. Brun P, Ghezzo F, Roso M, Danesin R, Palù G, Bagno A, Modesti M, Castagliuolo I, Dettin M (2011) Acta Biomater 7(6):2526
37. Pant HR, Neupane MP, Pant B, Panthi G, Oh H-J, Lee MH, Kim HY (2011) Colloid Surface B 88(2):587
38. Luo Y, Nartker S, Miller H, Hochhalter D, Wiederoder M, Wiederoder S, Setterington E, Drzal LT, Alocilja EC (2010) Biosens Bioelectron 26(4):1612
39. Anuradha S, Uma Maheswari K, Swaminathan S (2011) Biomed Mater 6(2):025004
40. Rho KS, Jeong L, Lee G, Seo B-M, Park YJ, Hong S-D, Roh S, Cho JJ, Park WH, Min B-M (2006) Biomaterials 27(8):1452
41. Teng S-H, Lee E-J, Wang P, Kim H-E (2008) Mater Lett 62(17–18):3055
42. Huang Z-M, Zhang YZ, Ramakrishna S, Lim CT (2004) Polymer 45(15):5361
43. Songchotikunpan P, Tattiyakul J, Supaphol P (2008) Int J Biol Macromol 42(3):247
44. Homayoni H, Ravandi SAH, Valizadeh M (2009) Carbohyd Polym 77(3):656
45. Geng X, Kwon O-H, Jang J (2005) Biomaterials 26(27):5427
46. Chen C, Chuanbao C, Xilan M, Yin T, Hesun Z (2006) Polymer 47(18):6322
47. Noh HK, Lee SW, Kim J-M, Oh J-E, Kim K-H, Chung C-P, Choi S-C, Park WH, Min B-M (2006) Biomaterials 27(21):3934
48. Min B-M, Lee SW, Lim JN, You Y, Lee TS, Kang PH, Park WH (2004) Polymer 45(21):7137
49. Zhao N, Shi S, Lu G, Wei M (2008) J Phys Chem Solids 69 (5–6):1564
50. Li D, Frey MW, Vynias D, Baeumner AJ (2007) Polymer 48(21):6340
51. Eugene D, Boland GEW, Simpson DavidG, Kristin J (2001) J Macromol Sci A 38(12):1231
52. You Y, Lee SW, Youk JH, Min B-M, Lee SJ, Park WH (2005) Polym Degrad Stabil 90(3):441
53. Wang Wang M, Hsieh AJ, Rutledge GC (2005) Polymer 46(10):3407
54. Wei S, Yu Y, Zhou M (2010) Mater Lett 64(21):2284
55. Yun S, Lim S (2011) J Solid State Chem 184(2):273
56. Yaakob Z, Jafar Khadem D, Shahgaldi S, Wan Daud WR, Tasirin SM (2012) Int J Hydrogen Energ 37(10):8388
57. Kanjwal MA, Sheikh FA, Barakat NAM, Li X, Kim HY, Chronakis IS (2012) Appl Surf Sci 258(8):3695
58. Sahay R, Sundaramurthy J, Suresh Kumar P, Thavasi V, Mhaisalkar SG, Ramakrishna S (2012) J Solid State Chem 186:261
59. Choi S-W, Park JY, Kim SS (2011) Chem Eng J 172(1):550
60. Yu J, Wang A, Tang Z, Henry J, Li-Ping Lee B, Zhu Y, Yuan F, Huang F, Li S (2012) Biomaterials 33(32):8062
61. Hassan MS, Amna T, Yang OB, Kim H-C, Khil M-S (2012) Ceram Int 38(7):5925
62. Song X, Zhang D, Fan M (2009) Appl Surf Sci 255(16):7343
63. Liu L, Guo C, Li S, Wang L, Dong Q, Li W (2010) Sensor Actuat B: Chem 150(2):806
64. Choi S-W, Zhang J, Akash K, Kim SS (2012) Sensor Actuat B: Chem 169:54

65. Kim HW, Kim HE, Knowles JC (2006) Adv Funct Mater 16(12):1529
66. Al-Munajjed AA, Plunkett NA, Gleeson JP, Weber T, Jungreuthmayer C, Levingstone T, Hammer J, O'Brien FJ (2009) Journal of Biomed Mater Res B 90B(2):584
67. Lee H–H, Yu H-S, Jang J-H, Kim H-W (2008) Acta Biomater 4(3):622
68. Noh K-T, Lee H-Y, Shin U-S, Kim H-W (2010) Mater Lett 64(7):802
69. Zhang Y, He X, Li J, Miao Z, Huang F (2008) Sensor Actuat B: Chem 132(1):67
70. Peng F, Yu X, Wei M (2011) Acta Biomater 7(6):2585
71. Chen J-P, Chang Y-S (2011) Colloid Surface B 86(1):169
72. Kim Hae-Won SJ-H, Kim Hyoun EE (2006) J Biomed Mater Res A 79(3):698
73. Fong ELS, Watson BM, Kasper KK, Mikos AG (2012) Adv Mater 24(35):4995
74. Rezwan K, Chen QZ, Blaker JJ, Boccaccini AR (2006) Biomaterials 27(18):3413
75. Nair LS, Laurencin CT (2007) Prog Pol Sci 32(8–9):762
76. Browning MB, Dempsey D, Guiza V, Becerra S, Rivera J, Russell B, Hook M, Clubb F, Miller M, Fossum T, Dong JF, Bergeron AL, Hahn M, Cosgriff-Hernandez E (2012) Acta Biomater 8(3):1010
77. Wang H, Feng Y, Fang Z, Yuan W, Khan M (2012) Mater Sci Eng, C 32(8):2306
78. Michiels Michiels C (2003) J Cell Physiol 196(3):430
79. de Mel A, Jell G, Stevens MM, Seifalian AM (2008) Biomacromolecules 9(11):2969
80. Zheng W, Wang Z, Song L, Zhao Q, Zhang J, Li D, Wang S, Han J, Zheng X-L, Yang Z, Kong D (2012) Biomaterials 33(10):2880
81. Hashi CK, Derugin N, Janairo RRR, Lee R, Schultz D, Lotz J, Li S (2010) Arterioscl Throm Vas 30(8):1621
82. Blit PH, Battiston KG, Yang M, Paul Santerre J, Woodhouse KA (2012) Acta Biomater 8(7):2493
83. Wise SG, Byrom MJ, Waterhouse A, Bannon PG, Weiss AS, Ng MK (2011) Acta Biomater 7(3):295
84. He W, Ma Z, Teo WE, Dong YX, Robless PA, Lim TC, Ramakrishna S (2009) J Biomed Mater Res A 90A(1):205
85. He W, Ma Z, Yong T, Teo WE, Ramakrishna S (2005) Biomaterials 26(36):7606
86. Zhu Y, Leong MF, Ong WF, Chan-Park MB, Chian KS (2007) Biomaterials 28(5):861
87. Ma Z, Kotaki M, Yong T, He W, Ramakrishna S (2005) Biomaterials 26(15):2527
88. Zhang M, Wang Z, Wang Z, Feng S, Xu H, Zhao Q, Wang S, Fang J, Qiao M, Kong D (2011) Colloids Surf B Biointerfaces 85(1):32
89. Liu H, Li X, Zhou G, Fan H, Fan Y (2011) Biomaterials 32(15):3784
90. Wang S, Zhang Y, Wang H, Dong Z (2011) Int J Biol Macromol 48(2):345
91. Du F, Wang H, Zhao W, Li D, Kong D, Yang J, Zhang Y (2012) Biomaterials 33(3):762
92. Liu B, Xu F, Guo MY, Chen SF, Wang J, Zhang B (2012) Surf Coat Tech http://dx.doi.org/10.1016/j.surfcoat.2012.03.033
93. Hoshi RA, Van Lith R, Jen MC, Allen JB, Lapidos KA, Ameer G (2013) Biomaterials 34(1):30
94. Lee J, Yoo JJ, Atala A, Lee SJ (2012) Biomaterials 33(28):6709
95. Hong Y, Ye S-H, Nieponice A, Soletti L, Vorp DA, Wagner WR (2009) Biomaterials 30(13):2457
96. de Valence S, Tille J-C, Mugnai D, Mrowczynski W, Gurny R, Möller M, Walpoth BH (2012) Biomaterials 33(1):38
97. Björn C, Mathilda Zetterström A, Ulf N, Johan L, Kuhn HG (2009) Biomed Mater 4(4):045004
98. Han Bing W, Michael EM, Jared MC, Andres H, Martin O, Matthew TT, Ryan JG (2009) J Neural Eng 6(1):016001
99. Lim SH, Liu XY, Song H, Yarema KJ, Mao H-Q (2010) Biomaterials 31(34):9031
100. Mey J, Brook G, Hodde D, Kriebel A (2012) In: Jayakumar R, Nair S (eds) Biomedical Applications of Polymeric Nanofibers, vol 246. Springer, Berlin, pp 131
101. Cho YI, Choi JS, Jeong SY, Yoo HS (2010) Acta Biomater 6(12):4725
102. Jiang X, Cao HQ, Shi LY, Ng SY, Stanton LW, Chew SY (2012) Acta Biomater 8(3):1290
103. Liu T, Xu J, Chan BP, Chew SY (2012) J Biomed Mater Res A 100A(1):236
104. Silver J, Miller JH (2004) Nat Rev Neurosci 5(2):146
105. Nicholas JS, Ryan JG (2011) J Neural Eng 8(4):046026
106. Wittmer CR, Claudepierre T, Reber M, Wiedemann P, Garlick JA, Kaplan D, Egles C (2011) Adv Funct Mater 21(22):4232
107. Prabhakaran MP, Ghasemi-Mobarakeh L, Jin G, Ramakrishna S (2011) J Biosci Bioeng 112(5):501
108. Xie J, MacEwan MR, Willerth SM, Li X, Moran DW, Sakiyama-Elbert SE, Xia Y (2009) Adv Funct Mater 19(14):2312
109. Lee JY, Bashur CA, Goldstein AS, Schmidt CE (2009) Biomaterials 30(26):4325
110. Li M, Guo Y, Wei Y, MacDiarmid AG, Lelkes PI (2006) Biomaterials 27(13):2705
111. Jeong SI, Jun ID, Choi MJ, Nho YC, Lee YM, Shin H (2008) Macromol Biosci 8(7):627
112. Veluru JB, Satheesh KK, Trivedi DC, Murthy VRamakrishna, Natarajan T (2007) J Eng Fiber Fabr 2(2):25
113. Chronakis IS, Grapenson S, Jakob A (2006) Polymer 47(5):1597
114. Yu Q-Z, Z-w Dai, Lan P (2011) Mat Sci Eng: B 176(12):913
115. Liu Y, Liu X, Chen J, Gilmore KJ, Wallace GG (2008) Chem Commun 32: 3729
116. Lee Y-S, Collins G, Livingston Arinzeh T (2011) Acta Biomater 7(11):3877
117. Weber N, Lee YS, Shanmugasundaram S, Jaffe M, Arinzeh TL (2010) Acta Biomater 6(9):3550
118. Bianco A, Di Federico E, Cacciotti I (2011) Polym for Advan Technol 22(12):1832
119. Prabhakaran MP, Venugopal J, Ramakrishna S (2009) Acta Biomater 5(8):2884
120. Ravichandran R, Venugopal JR, Sundarrajan S, Mukherjee S, Ramakrishna S (2012) Biomaterials 33(3):846
121. Yeo M, Lee H, Kim G (2010) Biomacromolecules 12(2):502
122. Phipps MC, Clem WC, Grunda JM, Clines GA, Bellis SL (2012) Biomaterials 33(2):524
123. Ren L, Wang J, Yang F-Y, Wang L, Wang D, Wang T-X, Tian M–M (2010) Mater Sci Eng, C 30(3):437
124. Molamma P, Prabhakaran JV, Ghasemi-Mobarakeh Laleh, Dan Kai GJ, Ramakrishna Seeram (2012) Adv Polym Sci 246:21
125. Guarino V, Alvarez-Perez M, Cirillo V, Ambrosio L (2011) J Bioact and Compat Pol 26(2):144
126. Bao C, Chen W, Weir MD, Thein-Han W, Xu HHK (2011) Acta Biomater 7(11):4037
127. Rim NG, Kim SJ, Shin YM, Jun I, Lim DW, Park JH, Shin H (2012) Colloid Surface B 91:189
128. Tambralli A, Blakeney B, Anderson J, Kushwaha M, Andukuri A, Dean D, Jun HW (2009) Biofabrication 1(2):025001
129. Martins A, Duarte AR, Faria S, Marques AP, Reis RL, Neves NM (2010) Biomaterials 31(22):5875
130. Ji W, Yang F, Ma J, Bouma MJ, Boerman OC, Chen Z, van den Beucken JJ, Jansen JA (2013) Biomaterials 34(3):735
131. Su Y, Su Q, Liu W, Lim M, Venugopal JR, Mo X, Ramakrishna S, Al-Deyab SS, El-Newehy M (2012) Acta Biomater 8(2):763
132. Wang Y, Gao R, Wang P–P, Jian J, Jiang X-L, Yan C, Lin X, Wu L, Chen G-Q, Wu Q (2012) Biomaterials 33(2):485

133. Qu J, Zhou D, Xu X, Zhang F, He L, Ye R, Zhu Z, Zuo B, Zhang H (2012) Appl Surf Sci 261:320
134. Li H, Wen F, Wong YS, Boey FY, Subbu VS, Leong DT, Ng KW, Ng GK, Tan LP (2012) Acta Biomater 8(2):531
135. Martins A, da Silva MLA, Faria S, Marques AP, Reis RL, Neves NM (2011) Macromol Biosci 11(7):978
136. Subramony SD, Dargis BR, Castillo M, Azeloglu EU, Tracey MS, Su A, Lu HH (2013) Biomaterials 34(8):1942
137. Nandakumar A, Tahmasebi Birgani Z, Santos D, Mentink A, Auffermann N, van der Werf K, Bennink M, Moroni L, van Blitterswijk C, Habibovic P (2013) Biofabrication 5(1):015006
138. Vines JB, Lim DJ, Anderson JM, Jun HW (2012) Acta Biomater 8(11):4053
139. Nie L, Chen D, Yang Q, Zou P, Feng S, Hu H, Suo J (2013) Mater Lett 92:25
140. Lee JH, Rim NG, Jung HS, Shin H (2010) Macromol Biosci 10:173
141. Chen JP, Chang YS (2011) Colloid Surface B 86:169
142. He C, Xiao G, Jin X, Sun C, Ma PX (2010) Adv Funct Mater 20:3568
143. So K, Fujibayashi S, Neo M, Anan Y, Ogawa T, Kokubo T, Nakamura T (2006) Biomaterials 27(27):4738
144. Jugdaohsingh R, Tucker KL, Qiao N, Cupples LA, Kiel DP, Powell JJ (2004) J Bone Miner Res 19(2):297
145. Carlisle EM (1972) Science 178(4061):619
146. Seaborn CD, Nielsen FH (2002) J Trace Elem Exp Med 15(3):113
147. Hench LL, Splinter RJ, Allen WC, Greenlee TK (1971) J Biomed Mater Res 5(6):117
148. Shirtliff VJ, Hench LL (2003) J Mater Sci 38(23):4697. doi: 10.1023/A:1027414700111
149. Labbaf S, Tsigkou O, Müller KH, Stevens MM, Porter AE, Jones JR (2011) Biomaterials 32(4):1010
150. Jones JR, Tsigkou O, Coates EE, Stevens MM, Polak JM, Hench LL (2007) Biomaterials 28(9):1653
151. Ebisawa Y, Kokubo T, Ohura K, Yamamuro T (1990) J Mater Sci: Mater M 1(4):239
152. Goh YF, Alshemary AZ, Akram M, Abdul Kadir MR, Hussain R (2013) Mater Chem Phys 137(3):1031
153. Arcos D, Vallet-Regí M (2010) Acta Biomater 6(8):2874
154. Alcaide M, Portolés P, López-Noriega A, Arcos D, Vallet-Regí M, Portolés MT (2010) Acta Biomater 6(3):892
155. Välimäki V–V, Moritz N, Yrjans JJ, Dalstra M, Aro HT (2005) Biomaterials 26(33):6693
156. Goudouri OM, Kontonasaki E, Theocharidou A, Papadopoulou L, Kantiranis N, Chatzistavrou X, Koidis P, Paraskevopoulos KM (2011) Mater Chem Phys 125(1–2):309
157. Elshahat A, Shermak MA, Inoue N, Chao EY, Manson P (2004) J craniofac surg 15(3):483
158. Merwin GE (1986) Ann Otol Rhinol Laryngol 95(1 Pt.1):78
159. Schrooten J, Helsen JA (2000) Biomaterials 21(14):1461
160. Fathi MH, Doostmohammadi A (2009) J Mater Process Tech 209(3):1385
161. Xia W, Zhang D, Chang J (2007) Nanotechnology 18(13):135601
162. Lu H, Zhang T, Wang X, Fang Q (2009) J. Mater. Sci. M 20(3):793
163. Kim J–J, Won J-E, Shin U-S, Kim H-W (2011) J. Amer. Ceram. Soc. 94(9):2812
164. Hong Y, Chen X, Jing X, Fan H, Guo B, Gu Z, Zhang X (2010) Adv Mater 22(6):754
165. Xie J, Blough E, Wang C-H (2012) Acta Biomater 8(2):811
166. Xia W, Chang J (2006) J Control Release 110(3):522
167. Jo J-H, Lee E-J, Shin D-S, Kim H-E, Kim H-W, Koh Y-H, Jang J-H (2009) J Biomed Mater Res B 91B(1):213
168. Fang Q, Denglong C, Zhiming Y, Min L (2009) Mater Sci Eng, C 29(5):1527
169. Xin X, Hussain M, Mao JJ (2007) Biomaterials 28(2):316
170. Liu H, Fan H, Wong Y, Toh SL, Goh JC (2008) Biomaterials 29(6):662
171. Fan H, Liu H, Wong EJ, Toh SL, Goh JC (2008) Biomaterials 29(23):3324
172. Fan H, Liu H, Toh SL, Goh JC (2009) Biomaterials 30(28):4967
173. Sahoo S, Ang L-T, Cho-Hong Goh J, Toh S-L (2010) Differentiation 79(2):102
174. Yin Z, Chen X, Chen JL, Shen WL, Hieu Nguyen TM, Gao L, Ouyang HW (2010) Biomaterials 31(8):2163
175. Lee CH, Shin HJ, Cho IH, Kang YM, Kim IA, Park KD, Shin JW (2005) Biomaterials 26(11):1261
176. Surrao DC, Fan JC, Waldman SD, Amsden BG (2012) Acta Biomater 8(10):3704
177. Surrao DC, Waldman SD, Amsden BG (2012) Acta Biomater 8(11):3997
178. Ladd MR, Lee SJ, Stitzel JD, Atala A, Yoo JJ (2011) Biomaterials 32(6):1549
179. Samavedi S, Olsen Horton C, Guelcher SA, Goldstein AS, Whittington AR (2011) Acta Biomater 7(12):4131
180. Samavedi S, Guelcher SA, Goldstein AS, Whittington AR (2012) Biomaterials 33(31):7727
181. Vaquette C, Kahn C, Frochot C, Nouvel C, Six J-L, De Isla N, Luo L-H, Cooper-White J, Rahouadj R, Wang X (2010) J Biomed Mater Res A 94A(4):1270
182. Sahoo S, Toh SL, Goh JCH (2010) Biomaterials 31(11):2990
183. Sahoo S, Ang LT, Goh JC-H, Toh S-L (2010) J Biomed MaterRes A 93A(4):1539
184. Soliman S, Sant S, Nichol JW, Khabiry M, Traversa E, Khademhosseini A (2011) J Biomed Mater Res A 96A:566
185. Lowery JL, Datta N, Rutledge GC (2010) Biomaterials 31(3):491
186. Karageorgiou V, Kaplan D (2005) Biomaterials 26(27):5474
187. Wright LD, Andric T, Freeman JW (2011) Mater Sci Eng, C 31(1):30
188. Leong MF, Rasheed MZ, Lim TC, Chian KS (2009) J Biomed Mater Res A 91(1):231
189. Blakeney BA, Tambralli A, Anderson JM, Andukuri A, Lim DJ, Dean DR, Jun HW (2011) Biomaterials 32(6):1583
190. Baker BM, Gee AO, Metter RB, Nathan AS, Marklein RA, Burdick JA, Mauck RL (2008) Biomaterials 29(15):2348
191. Galperin A, Long TJ, Ratner BD (2010) Biomacromolecules 11(10):2583
192. Yixiang D, Yong T, Liao S, Chan CK, Ramakrishna S (2008) Tissue Eng Part A 14(8):1321
193. Rnjak-Kovacina J, Wise SG, Li Z, Maitz PK, Young CJ, Wang Y, Weiss AS (2011) Biomaterials 32(28):6729
194. Vaquette C, Cooper-White JJ (2011) Acta Biomater 7(6):2544
195. Lee BL, Jeon H, Wang A, Yan Z, Yu J, Grigoropoulos C, Li S (2012) Acta Biomater 8(7):2648
196. Kurpinski KT, Stephenson JT, Janairo RR, Lee H, Li S (2010) Biomaterials 31(13):3536
197. Li L, Qian Y, Jiang C, Lv Y, Liu W, Zhong L, Cai K, Li S, Yang L (2012) Biomaterials 33(12):3428
198. Kim GH, Yoon H, Park YK (2010) Appl Phys A 100(4):1197
199. Jabal JMF, McGarry L, Sobczyk A, Aston DE (2009) ACS Appl Mater Interfaces 1(10):2325
200. Sun B, Long YZ, Yu F, Li MM, Zhang HD, Li WJ, Xu TX (2012) Nanoscale 4(6):2134
201. Jin L, Wang T, Zhang QF, Zhu M, Leach MK, Naim Y, Jiang Q (2012) J Mater Chem 22(35):18321
202. Yang W, Yang F, Wang Y, Both SK, Jansen JA (2013) Acta Biomater 9(1):4505

203. Rampichová M, Chvojka J, Buzgo M, Prosecká E, Mikeš P, Vysloužilová L, Tvrdík D, Kochová P, Gregor T, Lukáš D, Amler E (2012) Cell Prolif. doi:10.1111/cpr
204. Vaquette C, Cooper-White J (2012) Cell Tissue Res 347(3):815
205. Andric T, Wright LD, Taylor BL, Freeman JW (2012) J Biomed Mater Res A 100A(8):2097
206. Cai YZ, Zhang GR, Wang LL, Jiang YZ, Ouyang HW, Zou XH (2012) J Biomed Mater Res A 100A(5):1187
207. Leung LH, Naguib H (2012) J Appl Polym Sci 125(S2): E61
208. Vaquette C, Cooper-White J (2013) Acta Biomater 9(1):4599
209. Nam J, Huang Y, Agarwal S, Lannutti J (2008) J Appl Polym Sci 107(3):1547
210. Chen DW, Hsu YH, Liao JY, Liu SJ, Chen JK, Ueng SW (2012) Int J Pharm 430(1–2):335
211. Xing ZC, Chae WP, Huh MW, Park LS, Park SY, Kwak G, Yoon KB, Kang IK (2011) J Nanosci Nanotechnol 11(1):61
212. Chen ZG, Wang PW, Wei B, Mo XM, Cui FZ (2010) Acta Biomater 6(2):372
213. Nandakumar A, Fernandes H, de Boer J, Moroni L, Habibovic P, van Blitterswijk CA (2010) Macromol Biosci 10(11):1365
214. Zhang F, Zuo BQ, Bai L (2009) J Mater Sci 44(20):5682. doi:10.1007/s10853-009-3800-5
215. Zhang F, Zuo BQ, Zhang HX, Bai L (2009) Polymer 50(1):279
216. Dong B, Arnoult O, Smith ME, Wnek GE (2009) Macromol Rapid Commun 30(7):539
217. Chakrapani VY, Gnanamani A, Giridev VR, Madhusoothanan M, Sekaran G (2012) J Appl Polym Sci 125(4):3221
218. Jiang Q, Reddy N, Zhang S, Roscioli N, Yang Y (2012) J Biomed Mater Res A doi. doi:10.1002/jbm.a.34422
219. Zha Z, Teng W, Markle V, Dai Z, Wu X (2012) Biopolymers 97(12):1026
220. Mazalevska O, Struszczyk MH (2012) J Appl Polym Sci. doi:10.1002/app.38818
221. Shanmuganathan K, Sankhagowit R, Iyer P, Ellison C (2011) Chem Mater 23(21):4726
222. Janes DW, Shanmuganathan K, Chou DY, Ellison CJ (2012) ACS Macro Lett 1(9):1138
223. Langer R (1998) Nature 392(6679 Suppl):5
224. Verreck G, Chun I, Peeters J, Rosenblatt J, Brewster ME (2003) Pharmaceut Res 20(5):810
225. Saraf A, Baggett LS, Raphael RM, Kasper FK, Mikos AG (2010) J Control Release 143(1):95
226. Ji W, Yang F, van den Beucken JJJP, Bian Z, Fan M, Chen Z, Jansen JA (2010) Acta Biomater 6(11):4199
227. Meng ZX, Xu XX, Zheng W, Zhou HM, Li L, Zheng YF, Lou X (2011) Colloid Surface B: Biointerfaces 84(1):97
228. Yan J, Yu D-G (2012) J Mater Sci 47(20):7138. doi:10.1007/s10853-012-6653-2
229. Park CG, Kim E, Park M, Park J-H, Choy YB (2011) J Control Release 149(3):250
230. Shen X, Yu D, Zhu L, Branford-White C, White K, Chatterton NP (2011) Int J Pharm 408(1–2):200
231. Quan J, Yu Y, Branford-White C, Williams GR, Yu D-G, Nie W, Zhu L-M (2011) Colloid Surface B 88(1):304
232. Okuda T, Tominaga K, Kidoaki S (2010) J Control Release 143(2):258
233. Huang C, Soenen SJ, van Gulck E, Vanham G, Rejman J, Van Calenbergh S, Vervaet C, Coenye T, Verstraelen H, Temmerman M, Demeester J, De Smedt SC (2012) Biomaterials 33(3):962
234. Weldon CB, Tsui JH, Shankarappa SA, Nguyen VT, Ma M, Anderson DG, Kohane DS (2012) J Control Release 161(3):903
235. Yohe ST, Colson YL, Grinstaff MW (2012) Journal Am Chem Soc 134(4):2016
236. Yohe ST, Herrera VL, Colson YL, Grinstaff MW (2012) J Control Release 162(1):92
237. Thakur RA, Florek CA, Kohn J, Michniak BB (2008) Int J Pharm 364(1):87
238. Piras AM, Chiellini F, Chiellini E, Nikkola L, Ashammakhi N (2008) J Bioact Compat Pol 23:423
239. Beck-Broichsitter M, Thieme M, Nguyen J, Schmehl T, Gessler T, Seeger W, Agarwal S, Greiner A, Kissel T (2010) Macromol Biosci 10(12):1527
240. Xu J, Jiao Y, Shao X, Zhou C (2011) Mater Lett 65(17–18):2800
241. Qi H, Hu P, Xu J, Wang A (2006) Biomacromolecules 7(8):2327
242. Kriegel C, Kit KM, McClements DJ, Weiss J (2009) Part I: Fabrication and Characterization. Langmuir 25(2):1154
243. Yan S, Xiaoqiang L, Shuiping L, Xiumei M, Ramakrishna S (2009) Colloids Surf B Biointerfaces 73(2):376
244. Xu X, Chen X, Wang Z, Jing X (2009) Eur J Pharm Biopharm 72(1):18
245. Yang Y, Li X, Cui W, Zhou S, Tan R, Wang C (2008) J Biomed Mater Res A 86(2):374
246. Nie H, Wang CH (2007) J Control Release 120(1–2):111
247. Mickova A, Buzgo M, Benada O, Rampichova M, Fisar Z, Filova E, Tesarova M, Lukas D, Amler E (2012) Biomacromolecules 13(4):952
248. Zahedi P, Rezaeian I, Ranaei-Siadat SO, Jafari SH, Supaphol P (2010) Polym Advan Technol 21(2):77
249. Liu S-J, Kau Y-C, Chou C-Y, Chen J-K, Wu R-C, Yeh W-L (2010) J Membr Sci 355(1–2):53
250. Chong EJ, Phan TT, Lim IJ, Zhang YZ, Bay BH, Ramakrishna S, Lim CT (2007) Acta Biomater 3(3):321
251. Vargas EAT, do Vale Baracho NC, de Brito J, de Queiroz AAA (2010) Acta Biomater 6(3):1069
252. Schneider A, Wang XY, Kaplan DL, Garlick JA, Egles C (2009) Acta Biomater 5(7):2570
253. Miao J, Pangule RC, Paskaleva EE, Hwang EE, Kane RS, Linhardt RJ, Dordick JS (2011) Biomaterials 32(36):9557
254. Radetic M (2012) J Mater Sci. doi:10.1007/s10853-012-6677-7
255. Gunasekaran T, Nigusse T, Dhanaraju Magharla D (2012) J Am Col Certif Wound Spec. doi:10.1016/j.jcws.2012.05.001
256. Penchev H, Paneva D, Manolova N, Rashkov I (2010) Carbohyd Res 345(16):2374
257. Ma Z, Ji H, Tan D, Teng Y, Dong G, Zhou J, Qiu J, Zhang M (2011) Colloids Surface A 387(1–3):57
258. Shalumon KT, Anulekha KH, Nair SV, Nair SV, Chennazhi KP, Jayakumar R (2011) Int J Biol Macromol 49(3):247
259. Said SS, Aloufy AK, El-Halfawy OM, Boraei NA, El-Khordagui LK (2011) Eur J Pharm Biopharm 79(1):108
260. Said SS, El-Halfawy OM, El-Gowelli HM, Aloufy AK, Boraei NA, El-Khordagui LK (2012) Eur J Pharm Biopharm 80(1):85
261. Unnithan AR, Barakat NA, Pichiah PB, Gnanasekaran G, Nirmala R, Cha YS, Jung CH, El-Newehy M, Kim HY (2012) Carbohydr Polym 90(4):1786
262. Liu X, Lin T, Gao Y, Xu Z, Huang C, Yao G, Jiang L, Tang Y, Wang X (2012) J Biomed Mater Res B Appl Biomater 100B(6):1556
263. Li Y, Chen F, Nie J, Yang D (2012) Carbohydr Polym 90(4):1445
264. Wu L, Li H, Li S, Li X, Yuan X, Li X, Zhang Y (2010) J Biomed Mater Res 92A(2):563
265. Kang YO, Yoon IS, Lee SY, Kim DD, Lee SJ, Park WH, Hudson SM (2010) J Biomed Mater Res B Appl Biomater 92B(2):568
266. Liu X, Lin T, Fang J, Yao G, Zhao H, Dodson M, Wang X (2010) J Biomed Mater Res 94A(2):499
267. Jin G, Prabhakaran MP, Kai D, Annamalai SK, Arunachalam KD, Ramakrishna S (2013) Biomaterials 34(3):724
268. Xu C, Xu F, Wang B, Lu T (2011) J Nanomater 2911 Article ID 201834, 7 pp. doi:10.1155/2011/201834

269. Lakshman LR, Shalumon KT, Nair SV, Jayakumar R, Nair SV (2010) J Macromol Sci A 47(10):1012
270. Jao WC, Yang MC, Lin CH, Hsu CC (2012) Polym Adv Technol 23(7):1066
271. Hussain SM, Hess KL, Gearhart JM, Geiss KT, Schlager JJ (2005) Toxicol In Vitro 19(7):975
272. Shinde SK, Grampurohit ND, Gaikwad DD, Jadhav SL, Gadhave MV, Shelke PK (2012) Asian Pac J Trop Med 2(4):331
273. Karlsson HL, Gustafsson J, Cronholm P, Möller L (2009) Toxicol lett 188(2): 112
274. Spasova M, Manolova N, Paneva D, Mincheva R, Dubois P, Rashkov I, Maximova V, Danchev D (2010) Biomacromolecules 11(1):151
275. Kumar B, Vijayakumar M, Govindarajan R, Pushpangadan P (2007) J Ethnopharmacol 114(2):103
276. Selvaraj N, Lakshmanan B, Mazumder PM, Karuppasamy M, Jena SS, Pattnaik AK (2011) Asian Pac J Trop Med 4(12):959
277. Pattanayak SP, Sunita P (2008) J Ethnopharmacol 120(2):241
278. Adetutu A, Morgan WA, Corcoran O (2011) J Ethnopharmacol 133(1):116
279. Suwantong O, Ruktanonchai U, Supaphol P (2010) J Biomed Mater Res A 94(4):1216
280. Yarin AL, Zussman E (2004) Polymer 45(9):2977
281. Niu H, Lin T, Wang X (2009) J Appl Polym Sci 114(6): 3524
282. Zhou FL, Gong RH, Porat I (2009) Polym Eng Sci 49(12):2475
283. Lu B, Wang Y, Liu Y, Duan H, Zhou J, Zhang Z, Wang Y, Li X, Wang W, Lan W, Xie E (2010) Small 6(15):1612
284. Wang X, Xu W (2012) J Appl Polym Sci 123(6):3703
285. Wang X, Niu H, Wang X, Lin T (2012) J Nanomater. 2012:9 pp. Article ID 785920. doi:10.1155/2012/785920
286. Dubský M, Kubinová S, Širc J, Voska L, Zajíček R, Zajícová A, Lesný P, Jirkovská A, Michálek J, Munzarová M, Holáň V, Syková E (2012) J Mater Sci Mater Med 23(4):931